Atmos. Meas. Tech., 9, 2315–2333, 2016
www.atmos-meas-tech.net/9/2315/2016/
doi:10.5194/amt-9-2315-2016

Atmospheric Measurement Techniques
Open Access
EGU

Consistency and quality assessment of the Metop-A/IASI and Metop-B/IASI operational trace gas products (O_3, CO, N_2O, CH_4, and CO_2) in the subtropical North Atlantic

Omaira Elena García[1], Eliezer Sepúlveda[1], Matthias Schneider[2], Frank Hase[2], Thomas August[3], Thomas Blumenstock[2], Sven Kühl[1], Rosemary Munro[3], Ángel Jesús Gómez-Peláez[1], Tim Hultberg[3], Alberto Redondas[1], Sabine Barthlott[2], Andreas Wiegele[2], Yenny González[1], and Esther Sanromá[1]

[1]Izaña Atmospheric Research Centre (IARC), Agencia Estatal de Meteorología (AEMET), Santa Cruz de Tenerife, Spain
[2]Institute of Meteorology and Climate Research (IMK-ASF), Karlsruhe Institute of Technology (KIT), Karlsruhe, Germany
[3]European Organisation for the Exploitation of Meteorological Satellites (EUMETSAT), Darmstadt, Germany

Correspondence to: Omaira Elena García (ogarciar@aemet.es)

Received: 10 November 2015 – Published in Atmos. Meas. Tech. Discuss.: 21 December 2015
Revised: 10 May 2016 – Accepted: 12 May 2016 – Published: 25 May 2016

Abstract. This paper presents the tools and methodology for performing a routine comprehensive monitoring of consistency and quality of IASI (Infrared Atmospheric Sounding Interferometer) trace gas Level 2 (L2) products (O_3, CO, N_2O, CH_4, and CO_2) generated at EUMETSAT (European Organisation for the Exploitation of Meteorological Satellites) using ground-based observations at the Izaña Atmospheric Observatory (IZO, Tenerife). As a demonstration the period 2010–2014 was analysed, covering the version 5 of the IASI L2 processor. Firstly, we assess the consistency between the total column (TC) observations from the IASI sensors on board the EUMETSAT Metop-A and Metop-B meteorological satellites (IASI-A and IASI-B respectively) in the subtropical North Atlantic region during the first 2 years of IASI-B operations (2012–2014). By analysing different timescales, we probe the daily and annual consistency of the variability observed by IASI-A and IASI-B and thereby assess the suitability of IASI-B for continuation of the IASI-A time series. The continuous intercomparison of both IASI sensors also offers important diagnostics for identifying inconsistencies between the data records and for documenting their temporal stability. Once the consistency of IASI sensors is documented we estimate the overall accuracy of all the IASI trace gas TC products by comparing to coincident ground-based Fourier transform infrared spectrometer (FTS) measurements performed at IZO from 2010 to 2014. The IASI L2 products reproduce the ground-based FTS observations well at the longest temporal scales, i.e. annual cycles and long-term trends for all the trace gases considered (Pearson correlation coefficient, R, larger than 0.95 and 0.75 for long-term trends and annual cycles respectively) with the exception of CO_2. For CO_2 acceptable agreement is only achieved for long-term trends ($R \sim 0.70$). The differences observed between IASI and FTS observations can be in part attributed to the different vertical sensitivities of the two remote sensing instruments and also to the degree of maturity of the IASI products: O_3 and CO are pre-operational, while N_2O, CH_4, and CO_2 are, for the period covered by this study, aspirational products only and are not considered mature. Regarding shorter timescales (single or daily measurements), only the O_3 product seems to show good sensitivity to actual atmospheric variations ($R \sim 0.80$), while the CO product is only moderately sensitive ($R \sim 0.50$). For the remainder of the trace gases, further improvements would be required to capture the day-to-day real atmospheric variability.

Published by Copernicus Publications on behalf of the European Geosciences Union.

1 Introduction

Continuous, consistent, and high-quality long-term monitoring of the composition of the atmosphere is fundamental for addressing the challenges of climate research. In this context space-based remote sensing observations are of particular importance, since they are unique in providing a global coverage. Among the current space-based remote sensing instruments, IASI (Infrared Atmospheric Sounding Interferometer, Blumstein et al., 2004) has special relevance since it combines high quality (very good signal-to-noise ratio and high spectral resolution), good horizontal resolution (12 km at nadir), global coverage, and long-term data availability. Its mission is guaranteed until 2022 through the meteorological satellites Metop, the space component of the EUMETSAT (European Organisation for the Exploitation of Meteorological Satellites) Polar System (EPS) programme: the first sensor (IASI-A) was launched in October 2006 on board Metop-A, the second (IASI-B) was launched in September 2012 on board Metop-B, and the third (IASI-C) is expected to be launched in October 2018 aboard Metop-C. A successor to IASI, IASI-NG (Crevoisier et al., 2014), with improved spectral resolution and radiometric performance is under development as part of the EPS-SG (Second Generation) programme and will continue the mission after Metop-C and extend the data record by 2 decades. All these features make the IASI missions very promising for monitoring atmospheric composition in the long term as a key instrument for the EUMETSAT Earth observation programme (e.g. Clerbaux et al., 2009; Crevoisier et al., 2009a, b; Herbin et al., 2009; Schneider and Hase, 2011; August et al., 2012; Kerzenmacher et al., 2012). However, for correct scientific use of these long-term observational records, an assessment of the consistency of the atmospheric observations from the IASI sensors currently in orbit, as well as a documentation of their quality is required. To date there has been no comprehensive consistency and validation study for all the trace gas products disseminated by EUMETSAT as IASI Level 2 (L2) products. Such activities have been mostly performed in the context of short campaigns or have been focused on specific atmospheric parameters (e.g. Keim et al., 2009; Viatte et al., 2011; Schneider and Hase, 2011; García et al., 2013). By such campaigns alone it is not possible to extensively evaluate the quality of the different IASI atmospheric products as well as the potential of IASI for long-term climate studies. In order to address these two critical tasks, high-quality ground-based reference data sets are needed.

While there are several techniques for measuring total column (TC) amounts of atmospheric trace gases such as water vapour or ozone that can be used as a validation reference (e.g. radiosondes, UV–VIS spectrometers), there is currently only one technique that routinely estimates all the atmospheric trace gases retrieved operationally from IASI measurements (ozone, O_3, carbon monoxide, CO, nitrous oxide, N_2O, methane, CH_4, and carbon dioxide, CO_2): the ground-based Fourier transform spectrometers (FTSs). FTS instruments record very high-resolution infrared solar absorption spectra and use a similar measurement approach as IASI. By evaluating these solar spectra, the FTS systems can provide TC amounts and volume mixing ratio (VMR) profiles of many different atmospheric trace gases with high precision. Within the NDACC (Network for Detection of Atmospheric Composition Change, www.acom.ucar.edu/irwg/) such FTS experiments are operated at about 25 sites distributed worldwide. Since the 1990s, when these instruments began to be used for atmospheric composition monitoring, there have been continuous efforts to assure and even further improve the high quality of the FTS data products: monitoring the instrument line shape (e.g. Hase et al., 1999; Hase, 2012), monitoring and improving the accuracy of the solar trackers (e.g. Gisi et al., 2011), and developing and intercomparing sophisticated retrieval algorithms (e.g. Hase et al., 2004). The good quality of these long-term ground-based FTS data sets has been extensively documented by theoretical and empirical validation studies (e.g. Schneider et al., 2006, 2008; Sepúlveda et al., 2012; García et al., 2012b; Sepúlveda et al., 2014; Barthlott et al., 2015).

In this context this work intends to demonstrate monitoring capabilities for the IASI L2 atmospheric composition products, to help identifying potential areas for retrieval algorithm improvement, and to support the related ongoing and future development activities. For this purpose, it is firstly analysed the consistency between the IASI-A and IASI-B L2 atmospheric trace gas products provided by the IASI mission (TC amounts of O_3, CO, N_2O, CH_4, and CO_2) in the subtropical North Atlantic region after the 2 first years in operation of IASI-B (2012–2014). Secondly, the documentation of the overall IASI quality is addressed by using the high-precision FTS observations that have been carried out at the Izaña Atmospheric Observatory (IZO) since 1999. Due to its strategic location, IZO is affected by background free troposphere air masses with very distinct history and regions of origin (Atlantic Ocean, Europe, North and Central Africa, etc; see Cuevas et al., 2013, and references therein), making IZO a unique place for documenting the quality of IASI atmospheric products for different scenarios. To address all these tasks, this paper is structured as follows: Sect. 2 presents the EUMETSAT Metop/IASI mission describing the IASI sensor as well as the IASI L2 atmospheric trace gas products routinely disseminated by EUMETSAT, while Sect. 3 introduces the ground-based FTS products, including the FTS activities at IZO and the retrieval strategies used for obtaining the different FTS products. Section 4 presents the strategy developed for comparing IASI-A, IASI-B, and FTS observations and Sects. 5 and 6 address the consistency and intercomparison study at different timescales (single measurements, daily, annual, and long-term trends). Finally, Sect. 7 summarises the main results and conclusions of this work.

Table 1. Technical specifications of the IASI and IZO ground-based FTS instrument.

	IASI	Ground-based FTS
Instrument	Fourier transform spectrometer	Fourier transform spectrometer
Spectral range (cm^{-1})	645–2760	~ 740–9000
Apodized spectral resolution (cm^{-1})	0.5	0.005
Type of observation	Thermal emission of Earth–atmosphere	Solar absorption
Field of view (FOV)	50 km (3.33°) at nadir with four simultaneous pixels of 12 km	0.2° (FOV centred on solar disc)
Frequency of observation	twice per day ~ 10:30 and 21:30 UTC	continues observations during 2/3 days per week (weather permits)
Duration of observation	8 s (30 × 4 pixels)	~ 6–8 min
Data availability	2007–present	1999–present

2 EUMETSAT/IASI mission

2.1 IASI sensor

The IASI remote sensing instruments are nadir-viewing atmospheric sounders based on FTSs and developed by CNES (Centre National d'Etudes Spatiales, www.cnes.fr) in cooperation with EUMETSAT. They are on board the EUMETSAT Metop meteorological satellites, which operate in a polar, Sun-synchronous, low-Earth orbit since 2006 (Metop-A was launched in October 2006, Metop-B was launched in September 2012, and the Metop-C launch is scheduled for October 2018). The Metop-A and Metop-B currently operate in a co-planar orbit, 174° out of phase. The IASI sensors were designed with the main goal of retrieving operational meteorological soundings (temperature and humidity) with high vertical resolution and accuracy for weather forecast use, as well as for monitoring atmospheric composition (O_3, CO, N_2O, CH_4, and CO_2) at a global scale. Additionally, they provide land and sea surface temperature, surface emissivity, and cloud parameters (August et al., 2012). To do so, IASI records thermal infrared emission spectra of the Earth–atmosphere system in the 645–2760 cm^{-1} region (apodized spectral resolution of 0.5 cm^{-1}) with a surface swath width of about 2200 km twice per day. Table 1 provides the main IASI technical specifications and more information about these instruments can be found in Blumstein et al. (2004) and Clerbaux et al. (2009) (and references therein).

2.2 IASI operational trace gas products

Since 2008, when the first operational IASI data were delivered by the EUMETCast system (www.eumetsat.int), different versions of the IASI L2 Product Processing Facility (PPF) have been used to produce the EUMETSAT IASI L2 trace gas products: version 4 (V4) between June 2008 and September 2010, version 5 (V5) between September 2010 and September 2014, and version 6 (V6) from September 2014 onwards. Here we focus on the IASI V5 products, for which the longest IASI-A and coincident IASI-A and IASI-B time series are available (September 2010–September 2014 and December 2012–September 2014 respectively). The main characteristics of the IASI L2 V5 products are described below and summarised in Table 2.

Table 2. Description of the IASI L2 V5 trace gas products: spectral regions used for the retrievals, type of inversion algorithm (ANNs: artificial neural networks; OEM: optimal estimation method), status of the different products (Pre-Op: pre-operational; Aspi: aspirational), and target uncertainty within the IASI mission.

	Spectral region (cm^{-1})	Inversion method	Status	Target uncertainty (%)
O_3	1001–1065	OEM	Pre-op	5
CO	2111–2180	ANNs	Pre-op	≤ 10
N_2O	2200–2244	ANNs	Aspi	10–20
CH_4	1230–1347	ANNs	Aspi	10–20
CO_2	2050–2250	ANNs	Aspi	10–20

IASI L2 V5 introduces significant improvements in the retrieval of the atmospheric trace gas products as well as cloud products and cloud detection in contrast to the previous version, V4. Now, under cloud-free conditions, the O_3 profiles are simultaneously retrieved, together with the humidity and temperature profiles and the surface temperature, from the IASI measured radiances using an optimal estimation method (Rodgers, 2000). This approach uses a global a priori with a single unique covariance matrix, computed from a collection of ECMWF (European Centre for Medium-Range Weather Forecast) analysis records, independent on seasonal or latitudinal variations. Therefore, all observed atmospheric variability comes from the measurements rather than the a priori information (August et al., 2012).

The TC amounts of the other molecules (CO, N_2O, CH_4, and CO_2) are retrieved using an inversion algorithm based on artificial neural networks (ANNs). The feasibility of retrieving those quantities with ANNs from IASI measurements was first studied prior to launch (Turquety et al., 2004) and this formed the basis for the IASI L2 processors until revision V4. The method was refined in V5 specifically for CO with

an updated channel selection and the addition of new predictors adding important information about the surface characteristics and the viewing geometry (August et al., 2012). The ANNs were trained with simulated radiances using the RTTOV model (Matricardi and Saunder, 1999; Saunders et al., 1999) and the atmospheric composition profiles from the MOZART model (Brasseur et al., 1998). N_2O, CH_4, and CO_2 benefit from the same improvements in the ANNs design introduced for CO in V5, but they have not been specifically optimised and validated. They are only distributed as aspirational products while scientific development is ongoing and research products from the wider community (Clerbaux et al., 2009; Crevoisier et al., 2013) can be made operational.

The cloud screening strategy is key for the space-based atmospheric trace gas retrievals. For IASI L2 products, the cloud detection relies on five different cloud detection tests, based on the combined information of the measured IASI L1C spectra and of other remote sensors flying with IASI (AVHRR, AMSU, and ATOVS) as well as of comparison to synthetic radiances. An IASI pixel is flagged cloudy if at least one of the cloud tests detects the presence of clouds. For more details, refer to August et al. (2012) and the Products User Guide (EUM/OPSEPS/MAN/04/0033, EUMETSAT).

3 Ground-based FTS programme at the Izaña atmospheric observatory and FTS products

The IZO, run by the Izaña Atmospheric Research Centre (IARC, http://izana.aemet.es) belonging to the Spanish Meteorological Agency (AEMET), is a subtropical high-mountain observatory on Tenerife (Canary Islands, 28.3° N, 16.5° W, and 2373 m a.s.l.; Fig. 1), and only 350 km away from the African continent. It is usually well above the level of a strong subtropical temperature inversion layer, which acts as a natural barrier for local pollution. This fact, together with the quasi-permanent subsidence regime typical of the subtropical region, makes the air surrounding the observatory representative of the background free troposphere (particularly at night-time) (Gómez-Peláez et al., 2013; Cuevas et al., 2015, and references therein). These conditions are only significantly modified by episodes of mineral desert dust exports during summertime, when Saharan dust long-range transports within the so-called Saharan Air Layer (Prospero et al., 2002) are quite common (e.g. García et al., 2012a, and references therein). During wintertime, the Saharan events rarely reach the IZO altitude, since they are confined below 2 km of altitude (Díaz et al., 2006; Alonso-Pérez et al., 2011, and references therein).

Within the IZO's atmospheric research activities, the ground-based FTS measurements started in 1999 and continue until the present with two Bruker IFS spectrometers (an IFS 120M from 1999 to 2005 and an IFS 120/5HR from 2005 until present). These activities have contributed to the international networks NDACC and TCCON (Total Carbon Column Observing Network, www.tccon.caltech.edu) since 1999 and 2007 respectively. The FTS experiment at IZO records highly resolved infrared solar absorption spectra from 740 to 9000 cm^{-1}. However, in order to be consistent with the spectral range covered by IASI, for this study we only work with those measured in the middle infrared spectral region, i.e. between 740 and 4250 cm^{-1} (corresponding to the standard NDACC measurements). These solar spectra are acquired at an apodized spectral resolution of 0.005 cm^{-1}. Table 1 lists the main FTS characteristics and highlights the main differences and similarities between IASI and these ground-based FTS instruments. For further details about the FTS instrument at IZO refer to Schneider et al. (2005); Sepúlveda et al. (2012); García et al. (2012b, and references therein).

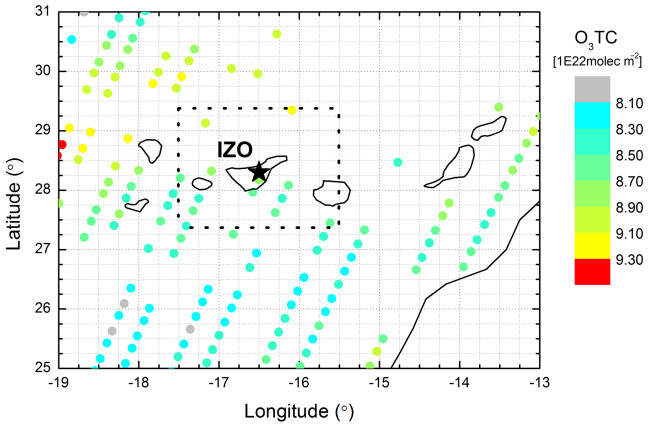

Figure 1. Site map indicating the location of the Izaña Atmospheric Observatory (IZO, marked by a black star) in the Canary Islands and the collocation box used for comparison (dashed lines), i.e. ±1° latitude/longitude centred at IZO location. The grid lines divide the area into boxes of 0.25°. Coloured filled circles correspond to IASI-A ozone total column observations on 31 January 2012.

The high-resolution FTS solar absorption spectra allow an observation of the pressure broadening effect and thus the retrieval of trace gas VMR profiles. In this work the target gas VMR profiles are retrieved using the algorithm PROFFIT (PROFile FIT; Hase et al., 2004) which follows the formalism given by Rodgers (2000). Then, TC amounts are computed by integrating the retrieved VMR profiles from the FTS altitude (2373 m a.s.l. for IZO) to the top of the atmosphere. For all the target gases considered we use a nearly identical retrieval strategy, which is summarised in Table 3. The target gas VMR profiles are retrieved using specific microwindows, also taking into account the absorption signatures of those trace gases interfering with the target gas (see Table 3). For O_3 and N_2O, the retrieval has also been refined by including a simultaneous temperature fit, which significantly reduces the error (Schneider et al., 2008; O. E. García et al., 2014). For this purpose, we add additional micro-windows containing well-isolated CO_2 lines.

Table 3. Description of the FTS retrieval setups used in this work. The profile retrieval is done by using a Tikhonov–Phillips slope constraint (TP1), while the scale retrieval corresponds to a scale to the a priori VMR profile. A summary of the error estimation is also provided: theoretical total systematic (SY) and statistical (ST) errors for the FTS total column products (median, $1\sigma \times 10^{-1}$, being σ the standard deviation of the error distributions between 2010 and 2014). XN_2O, XCH_4, and XCO_2 correspond to the total column-averaged dry air mole fractions of N_2O, CH_4, and CO_2 respectively.

	O_3	CO	N_2O	CH_4	CO_2
Spectral range (cm^{-1})	1001–1014	2057–2160	2481–2541	2611–2943	2620–2630
Inversion method	TP1	TP1	TP1	TP1	Scale
Temp. retrieval	Yes	No	Yes	No	No
Spectral range (cm^{-1})	962–970	–	2610–2627	–	–
Interfering species	H_2O, CO_2, C_2H_4	H_2O, CO_2, O_3 N_2O, OCS	H_2O, CO_2, O_3 CH_4	H_2O, HDO, CO_2, O_3 N_2O, NO_2, HCl, OCS	H_2O, CH_4
Theoretical SY (%)	2.0, 0.1	2.1, 0.4	2.1, 0.1	2.3, 0.1	3.5, 0.4
Theoretical ST (%)	0.4, 0.3	0.5, 0.1	0.2, 0.3	0.3, 0.3	0.6, 1.4
Experimental ST (%)	0.4–0.7	–	$\sim$0.4 in XN_2O	$\sim$1 in XCH_4	0.4 in XCO_2
References	Schneider et al. (2008) García et al. (2012b)	Barret et al. (2003) Velazco et al. (2007)	Angelbratt et al. (2011) O. E. García et al. (2014)	Sepúlveda et al. (2012, 2014)	Barthlott et al. (2015)

In order to reduce the interference error due to water vapour (the main interfering gas), we firstly perform a pre-fit of H_2O and in a second step simultaneously perform the target gas profile retrieval and a scale retrieval of all the interfering species considered. For all the target gases, the VMR profiles are retrieved on a logarithmic scale using an ad hoc Tikhonov–Phillips slope constraint (TP1 constraint), with the exception of CO_2, which is scaled to the a priori profile on a linear scale. The a priori profiles are taken from WACCM (Whole Atmosphere Community Climate Model-version 6, http://waccm.acd.ucar.edu) provided by NCAR (National Center for Atmospheric Research; J. Hannigan, private communication, 2014), averaged between 2008 and 2014 (period of IASI data). As a priori temperature we use the NCEP (National Centers for Environmental Prediction) 12:00 UTC daily temperature profiles. Note that only the a priori temperature profiles are updated daily. For all the target gases the a priori information is always kept constant; i.e. it does not vary on a daily or seasonal basis. Therefore, similarly to IASI, all the observed variability directly comes from the measured FTS spectra. Regarding spectroscopy, the spectroscopic line parameters are taken from HITRAN 2008 database (Rothman et al., 2009) including 2009 and 2012 updates (www.cfa.harvard.edu/hitran) for all the gases except for CH_4. For CH_4 we use a preliminary line list provided by D. Dubravica and F. Hase, obtained within a current project of the Deutsche Forschungsgemeinschaft, IUP Bremen, DLR Oberpfaffenhofen, and KIT, which has demonstrated lower spectroscopic residuals than the HITRAN 2008 linelist (Dubravica et al., 2013).

The FTS spectra are only recorded when the line of sight between the instrument and the Sun is cloud free. However, to avoid possible contamination of thin clouds, the FTS observations are, in a second step, filtered according to co-located global solar radiation observations taken at IZO in the framework of the Baseline Solar Radiation Network (BSRN, http://bsrn.awi.de). By using a cloud detection method on the coincident solar radiation measurements (based on Long and Ackerman, 2000, and adapted for IZO by R. D. García et al., 2014), the cloud-free periods in the FTS records are easily identified. Once the FTS retrievals are computed, they are filtered in a third step according to (i) the number of iterations at which the convergence is reached and (ii) the residues of the simulated–measured spectrum comparison. This final step ensures that unstable or imprecise FTS retrievals can be considered (which could likely be introduced by remaining thin clouds).

It is important to remark that the FTS products used here contain further refinements over the standard NDACC approaches (NDACC/Infrared Working Group, IRWG, www.acom.ucar.edu/irwg/) and, thus, they do not correspond to the FTS products publicly available at the NDACC archive. Refer to the references given in Table 3 for further details about the specific retrieval strategies used in this work.

Theoretically, the error of the different FTS products can be estimated by following the formalism detailed by Rodgers (2000) where three types of error can be distinguished: the smoothing error associated with the limited vertical sensitivity of the FTS instruments, the errors due to uncertainties in the input/model parameters (instrumental characteristics, spectroscopy data, etc), and the measurement noise. Using the error estimation as provided by PROFFIT and assuming the error sources and values listed in Appendix A, where the theoretical error estimation of the FTS products is detailed, the total statistical errors for the FTS TC products range from 0.2 to 0.6 %, while the systematic error is between 2 and 4 % (Table 3).

At IZO, other different high-quality measurement techniques for monitoring atmospheric trace gases are available (Cuevas et al., 2015). By using those data, a continuous em-

pirical documentation of the quality and long-term consistency of our FTS products has been carried out since the FTS instrument was installed at IZO in 1999. The FTS precision obtained from these experimental studies for the trace gases considered here is also listed in Table 3, showing a rather good agreement between theoretical and experimental errors.

4 Comparison strategy

4.1 Temporal decomposition

The consistency and quality assessment of IASI-A and IASI-B products is addressed at different timescales: single measurements, daily, annual, and long-term trends. This temporal decomposition provides an added value for validating trace gases with a rather small variability, such as N_2O or CO_2. For such gases the uncertainty is often larger than the day-to-day concentration variations and thus a validation at longer temporal scales is more meaningful than a validation limited to a comparison of individual measurements. Moreover, this analysis allows us to quickly detect instrumental issues or inconsistencies. For this purpose, we follow the procedure proposed by Sepúlveda et al. (2014) (and references therein), explained in detail in the following. Firstly, for analysing the time series on different timescales the measured TC time series of each target gas ($[TC]_{gas}$) is fitted to a time series model, which considers a mean $[TC]_{gas}$ value and $[TC]_{gas}$ variations on two different timescales (see Eq. 1): a linear trend and intra-annual variations.

$$F(t) = f_o + f_{\text{trend}}t + \sum_{i=1}^{p} [a_i \cos(\omega_i t) + b_i \sin(\omega_i t)], \qquad (1)$$

where t is measured in years, f_o is a baseline constant, and f_{trend} the linear trend in change per year. The annual cycle is modelled in terms of a Fourier series where a_i and b_i are the parameters of the Fourier series to be determined and $\omega_i = 2\pi i/T$ with $T = 365.25$ days. Once the model fit is computed, the seasonal variations are obtained by subtracting the fitted linear trends from the measured time series. The averaged annual cycle is then computed by averaging these de-trended time series on a monthly basis. It represents the de-trended multi-annual seasonal cycle of the target gas. In addition to the seasonal timescale we look on measurement-to-measurement and long-term timescales. For the separation into these two timescales we use the aforementioned time series model. The measurement-to-measurement timescale signal is calculated as the difference between the measured time series and the modelled time series (whereby all fitted timescales are considered: mean value, linear trend, and seasonal cycle). The so-calculated de-trended and de-seasonalised time series represents the very short-term variations, corresponding to the variations among individual observations. Finally, in order to calculate the long-term timescale signal (annual means) we reconstructed a time series that only considers the fit results obtained for the mean $[TC]_{gas}$ and the seasonal cycle. Then, by subtracting it from the measured time series, we get a de-seasonalised time series, for which we then calculate the annual mean values. Note that for IASI-A and IASI-B consistency study, the bias between both IASI sensors is also calculated. To do so, we directly compare the measured TCs of all the trace gases and compute the median difference of this difference time series.

This temporal decomposition has been done on a logarithmic scale, i.e. our measured time series correspond to the logarithm of the measured TCs of all the trace gases. This approach has two clear advantages in the subsequent IASI–FTS comparison: (i) the $[TC]_{gas}$ variations on this scale can be interpreted as variations relative to the reference mean values ($\Delta \ln[TC]_{gas} \approx \Delta[TC]_{gas}/[TC]_{gas}$) and we thereby directly compare the anomalies observed by both remote sensing instruments, and (ii) the relative differences between IASI and FTS observations can directly be computed as the subtraction of the corresponding variability on the different timescales (note that the temporal decomposition produces values very close to zero, thereby computing the standard relative differences provides very extreme values in some cases).

Table 4. Summary of the temporal and spatial collocation criteria adopted for each trace gas. Also shown are the typical degree of freedom for signal (DOFS) for IASI and FTS products, and the number of coincident observations between IASI and FTS (N). For IASI, the expected DOFS for O_3 and CO are taken from the Products User Guide (EUM/OPSEPS/MAN/04/0033, EUMETSAT), while for CH_4, N_2O, and CO_2 those are obtained from Turquety et al. (2004) and Clerbaux et al. (2009). The FTS DOFS are calculated from the corresponding retrievals between 2010 and 2014 (median $\pm 1\sigma$). Note that daily means 24 h means.

	Temporal and spatial collocation	IASI DOFS	FTS DOFS	N
O_3	± 1 h, $\pm 1°$	3–4	4.3 ± 0.1	2338
CO	± 1 h, $\pm 1°$	1–2	3.1 ± 0.1	2003
N_2O	Daily, $\pm 1°$	< 1	2.6 ± 0.1	425
CH_4	Daily, $\pm 1°$	1	2.2 ± 0.2	425
CO_2	Daily, $\pm 1°$	< 1	1*	425

* Scaled to the a priori VMR profile.

4.2 Collocation criteria

IASI and ground-based FTS instruments are sensing areas of different size and the acquisition times are generally not exactly simultaneous. In addition, both instruments have different vertical sensitivities. All these features have to be taken into account in the definition of the comparison strategy that, on the one hand, ensures the representativeness of the reference FTS data and, on the other hand, accounts for the spatial and temporal variability of the trace gases considered.

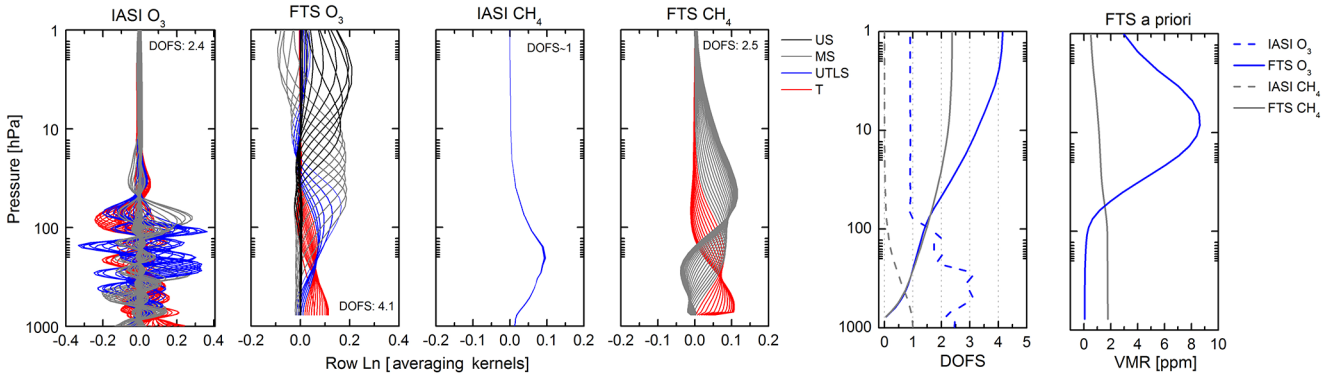

Figure 2. Row averaging kernels for O_3 and CH_4 as observed by IASI-A and FTS instruments, expressed on logarithm scale, for typical measurement conditions at IZO. US is upper stratosphere, MS is middle stratosphere, UTLS is upper troposphere and lower stratosphere, and T is troposphere. Also shown are the total degree of freedom for signal (DOFS), the vertical profile of the cumulative DOFS, as well as the a priori VMR profiles used for the FTS retrievals.

The collocation criteria selected are the result of a compromise between the spatial and temporal variability of each trace gas and the uncertainties and spatial range covered by the FTS observations and therefore can vary from gas to gas. Appendix B describes in detail the methodology followed to define the optimal coincidence criteria adopted for each trace gas, summarised in Table 4. In summary, we consider all the IASI observations within the box $\pm 1°$ latitude/longitude centred at the IZO location (Fig. 1) and pair those IASI and FTS observations taken within ± 1 h for O_3 and CO, and we pair daily median observations corresponding to the same day for the rest of trace gases. As previously mentioned, we consider all the TC observations disseminated in V5: September 2010–September 2014 for IASI-A and December 2012–September 2014 for IASI-B. From this data set we only work with the best quality IASI L2 V5 measurements: over sea, cloud free, and with the highest level of quality and completeness of the IASI retrieval as indicated in the Products User Guide (EUM/OPSEPS/MAN/04/0033, EUMETSAT).

For the consistency study between both IASI sensors (IASI-A and IASI-B) the 2° square has been divided in boxes of $\pm 0.25°$. Moreover, we distinguish between daily morning (10:00–11:00 UTC) and daily evening (22:00–23:00 UTC) TC observation overpasses in order to carefully analyse a possible bias for each overpass. Then, we compare TC amounts from each overpass and sensor for the same day. Note that for this study the IASI observations are paired without forcing temporal coincidence with the FTS data.

4.3 Vertical sensitivity

The vertical sensitivity of a remote sensing spectrometer depends, among other things, on the geometry of observations, the target gas considered as well as the specific characteristics of each instrument (e.g. the signal to noise ratio, spectral resolution). Hence, the responses of IASI and FTS to real atmospheric variability are significantly different. This fact can be observed in Fig. 2, where the rows of the IASI and FTS averaging kernels (**A**) are displayed for O_3 and CH_4. The IASI **A** are not operationally disseminated in V5; therefore, to illustrate its vertical sensitivity, we have taken the O_3 **A** from the EUMETSAT/IASI L2 version 6 products (EPS Product Validation Report: IASI L2 PPF v6, EUM/TSS/REP/14/776443 v4C, EUMETSAT), while the IASI CH_4 **A** have been obtained in the framework of the European project MUSICA (Schneider et al., 2013). Note that the rows of **A** describe the altitude regions that mainly contribute to the retrieved VMR profile and therefore these kernels can be used to identify the independent layers without significant overlap with other layers. Indeed, the trace of **A** (so-called the degrees of freedom for signal, DOFS) is a measure of the number of independent layers retrieved from the remote sensing measurements. Also, Fig. 2 includes the vertical profiles of the cumulative DOFS, calculated from the top of the atmosphere to surface for IASI and inversely for FTS as well as the a priori VMR used for the FTS retrievals in order to compare with the vertical sensitivity of the two remote sensing instruments.

Figure 2 illustrates two relevant facts that have to be taken into account when comparing IASI and FTS observations. First, IASI has a lower number of DOFS than FTS and the maximum sensitivity within these detected layers is located at different altitudes. Therefore, the TC amounts observed by both instruments could differently reflect the atmospheric composition variability. For example, when retrieving CH_4, IASI only detects one CH_4 layer (DOFS ~ 1), located in the upper troposphere/tropopause region ($\sim$ 12–14 km), while the FTS system detects two independent CH_4 partial columns (DOFS ~ 2.5), corresponding to the troposphere and the stratosphere. Similar conclusions might be derived for N_2O and CO (see, for example, Fig. 2 of Kerzenmacher et al., 2012). For O_3, the difference between the vertical sensitivities is not so significant and IASI is expected to

be sensitive to the maximum O_3 concentrations in the Chapman layer and to the tropopause/upper troposphere regions (DOFS $\sim$ 2.5). The expected IASI DOFS and the obtained FTS DOFS for all the trace gases are also listed in Table 4. The second important fact is that IASI has a weak sensitivity in the lower troposphere for the trace gases considered in this study, leading to the variability of the partial columns missed by FTS below 2373 m a.s.l. (IZO altitude) not being crucial for the IASI–FTS comparison.

5 Consistency between IASI-A and IASI-B observations

In order to probe the continuity provided by IASI-B as well as the consistency of each individual IASI sensor, it is indispensable to first analyse the temporal stability of their observations. For this purpose, we examine possible drifts and discontinuities in the times series of the differences between the de-seasonalised variability from IASI-A and IASI-B averaged on a weekly basis. The drift is defined as the linear trend in the differences, while the change points (changes in the weekly median of the difference time series) are analysed by using a robust rank order change-point test (Lanzante, 1996; O. E. García et al., 2014). By using these tools, we observe that the time series of the differences between the observations from the morning and evening overpasses for each IASI sensor as well as between the observations from the two sensors for each overpass are homogenous for all the trace gases considered (i.e. no change points were detected at 95 % confidence level). Moreover, all the difference time series reveal no significant drifts at 95 % confidence level. Figure 3 shows the time series of O_3 TC as observed by IASI-A and IASI-B and the corresponding differences.

This temporal stability study is complemented by analysing whether the distributions of the IASI-A and IASI-B observations could be statistically considered equivalent. To do so, we have used the Friedman non-parametric test, which detects differences in the distributions of related variables by checking the null hypothesis that multiple dependent samples come from the same statistical population (Sawilowsky and Fahoome, 2005). By applying this test on the observed short-term variability time series from the two IASI sensors for each overpass, which can be considered as four related samples for each trace gas, we only observe significant differences for the O_3 distributions between evening and morning overpasses (at 95 % confidence level). Nonetheless, these discrepancies disappear when comparing the observations for the same overpass; therefore, the IASI sensors distinguish the O_3 intra-day concentration variations. Indeed, for this trace gas the agreement between both sensors for the same overpass is significantly better than between the two overpasses for each sensor, as observed in Fig. 4, which displays the scatter plots between the O_3 de-trended and de-seasonalised variability as observed by the two IASI sensors for each overpass.

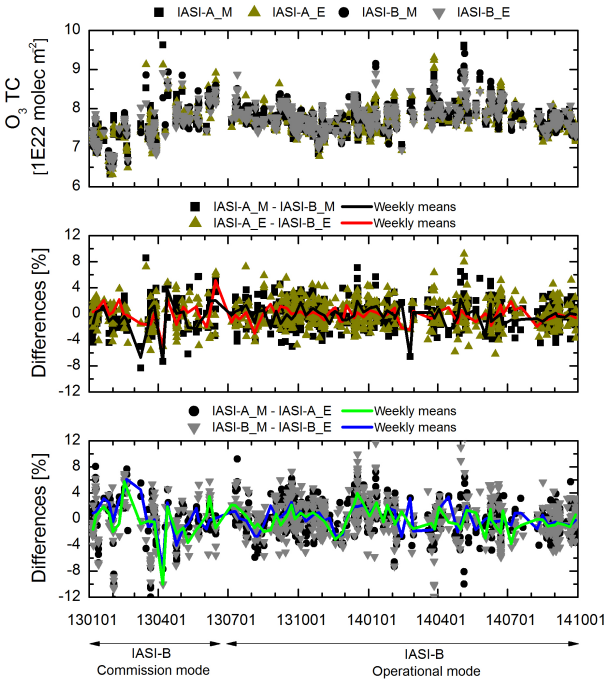

Figure 3. Time series of O_3 TC amounts (in 1×10^{22} molec m^{-2}) from the IASI-A and IASI-B overpasses (morning, M, and evening, E) (upper panel) and of the differences between the corresponding de-seasonalised variability (in %) for the morning and evening overpasses (middle and bottom panels). The solid lines represent the difference time series averaged on a weekly basis. The arrows distinguish the IASI-B commission mode (from 19 December 2012 to 18 June 2013) and the IASI-B operational mode (from 19 June 2013 onwards).

All of these findings suggest that, on the one hand, the observations from each sensor are consistent with themselves and, on the other hand, both sensors similarly reproduce the atmospheric composition variations. The statistics for the IASI-A and IASI-B intercomparison are summarised in Fig. 5 (Pearson correlation coefficient and standard deviation of the de-trended and de-seasonalised differences, and median bias). In summary, we observe that both IASI sensors similarly reproduce the annual cycle of all the trace gases considered ($R > 0.95$ except for CO_2, for which we observe a poorer agreement, $R \sim 0.70$–0.85), while for the very short-term concentration variations we find a large correlation for O_3 ($\sim$ 0.80) and moderate for the rest of trace gases ($R \sim 0.30$–0.60). The scatter (1σ) of the differences among sensors and overpasses, on a measurement-to-measurement basis, is less than 10 % for CO, $\sim$ 2 % for O_3 and between 1 and 2 % for the rest of the trace gases, while it decreases when comparing annual cycles: 2 % for CO, less than 0.5 % for the rest of trace gases. Regarding the biases between the IASI sensors (IASI-A–IASI-B), the values of ~ -3 % for

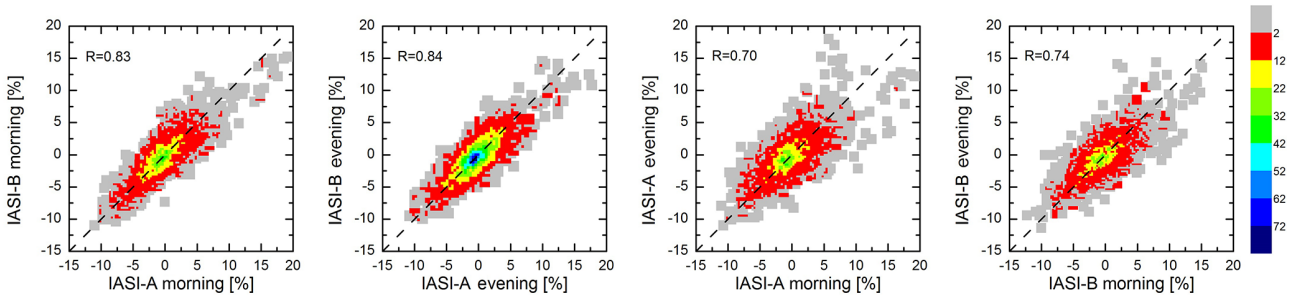

Figure 4. Scatter plots of the de-trended and de-seasonalised variability (in %) from the IASI-A and IASI-B overpasses (morning and evening) for O_3. The legend shows the Pearson correlation coefficient, R, and the colour bar indicates the number of coincident data per bin. The dashed lines represent the diagonals ($x = y$).

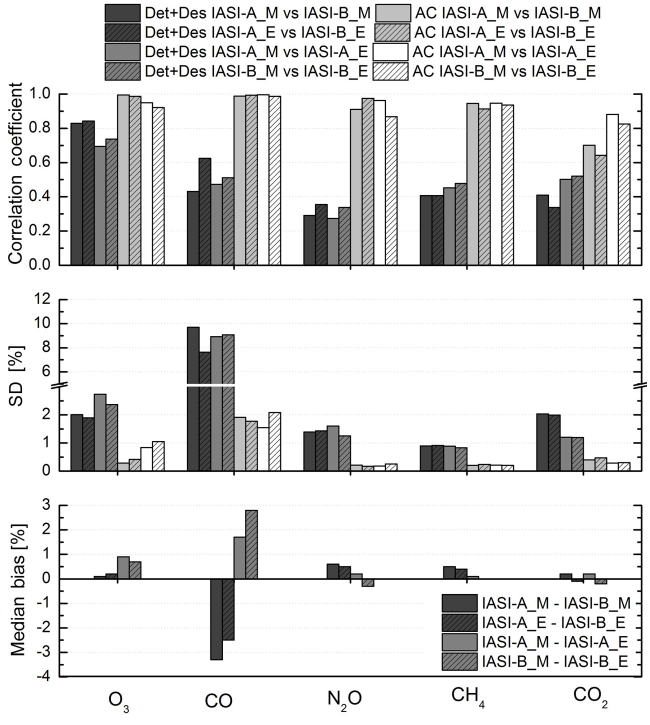

Figure 5. Pearson correlation coefficient (upper panel) between the observations from IASI-A and IASI-B overpasses (morning, M, and evening, E) for all the trace gases considered at different timescales: single measurements (de-trended and de-seasonalised variability, Det + Des) and annual cycle (AC). Middle panel shows the same, but for the standard deviation (in %) of the corresponding differences, while the bottom panel displays the median bias (in %). The number of coincident observations is 675.

CO and between 0.4 and 0.6 % for N_2O and CH_4 are remarkable (bottom panel in Fig. 5). For O_3 and CO_2 the bias is lower than 0.2 % in absolute value.

6 Comparison between IASI and ground-based FTS observations

This section presents the IASI–FTS comparison at different timescales: single measurements, daily, annual, and long-term trends. An example of this strategy is displayed in Fig. 6 for O_3, while the summary of the intercomparison results for all the trace gases is shown in Fig. 7 (Pearson correlation coefficient and standard deviation of the differences between IASI and FTS products). The consistency between both IASI sensors has been documented in the previous section. Therefore, here we only focus on IASI-A since it has the longest time series of measurements (September 2010–September 2014 for V5) as well as to ensure a homogeneous sampling during the whole period analysed.

As observed in Fig. 7, IASI reproduces the ground-based FTS observations well at the longest temporal scales, i.e. annual cycles and long-term trends. For the latter the correlation is larger than 0.95 for all the trace gases with the exception of CO_2 ($R \sim 0.70$), while on an annual basis, the correlation is larger than 0.95 for O_3 and CO and between 0.75 and 0.85 for CH_4 and N_2O. The discrepancies found for the annual cycles (amplitude and phase) can be explained by the different sensitivity of IASI and ground-based FTS instruments. As observed in Figs. 6c and 8, for O_3 and CO the IASI and FTS annual cycles are completely in phase, but the peak-to-peak amplitude is slightly different. For O_3 the largest differences are observed during spring–early summer due to the missing sensitivity of IASI in the troposphere and in part in the tropopause region (recall Fig. 2), while for CO we observe that IASI tends to overestimate the variability observed by the FTS. For CH_4 and N_2O the results are very similar: we observe that IASI products follow the annual shift of the tropopause altitude, where the maximum IASI sensitivity is located, and while FTS also reflects that annual shift, it is also sensitive to the tropospheric and stratospheric CH_4 and N_2O variations. As a consequence, the annual cycles observed by both remote sensors are slightly out of phase. For CO_2 the annual cycles are not correlated either in phase or in amplitude. This is likely due to the algorithm used in

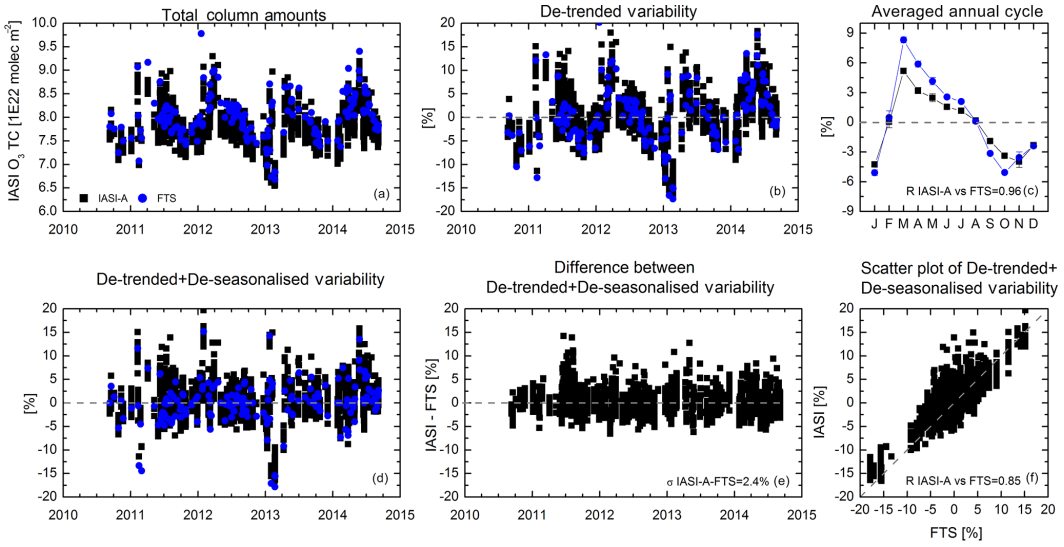

Figure 6. Summary of the IASI-A and FTS comparison for O_3: **(a, b)** time series of the TC amounts (in 1×10^{22} molec m^{-2}) and the de-trended variability (in %) respectively; **(c)** averaged annual cycle; **(d, e)** time series of the de-trended+de-seasonalised variability (in %), and the difference between coincident de-trended+de-seasonalised variability from IASI-A and FTS (in %) respectively; and **(f)** scatter plot of the de-trended + de-seasonalised variability. For **(c)** and **(f)** the Pearson correlation coefficient is included in the legends and for **(e)** the standard deviation of the differences. The number of coincident measurements is 2338.

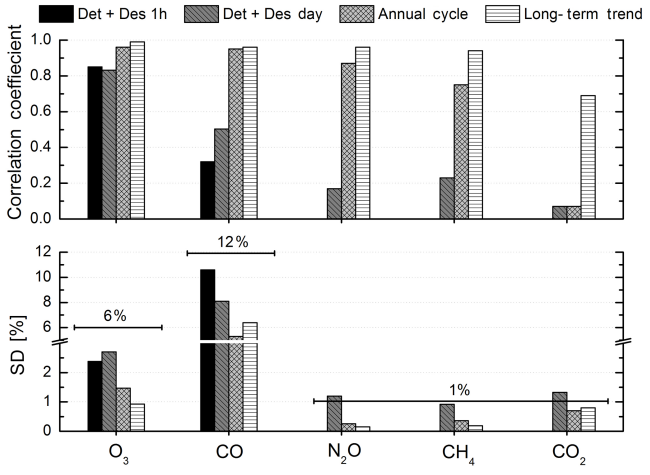

Figure 7. Pearson correlation coefficient (upper panel) between IASI-A and FTS observations for all the trace gases considered at different timescales: single measurements (de-trended + de-seasonalised variability within ±1 h, Det + Des 1 h), daily (de-trended + de-seasonalised variability within the same day, Det + Des Day), annual, and long-term trend. The number of coincident data is 2338 for O_3, 2003 for CO, and 425 for N_2O, CH_4, and CO_2. Bottom panel shows the same, but for the standard deviation (in %) of the corresponding differences. The solid black lines represent the day-to-day variability calculated from the FTS observations at IZO between 2010 and 2014.

the IASI L2 processor which has not been specifically optimised for CO_2, since the middle infrared FTS CO_2 products have successfully proven their reliability to monitor the CO_2 concentrations (Barthlott et al., 2015). In particular, the IASI CO_2 retrieval is solely based on the IASI measurements unlike in Crevoisier et al. (2009a), where collocated microwave measurements are exploited together with IASI data to disentangle the temperature and the CO2 signals in the thermal infrared spectra.

For the shortest-term variations we find poorer agreements, although the correlation is significantly larger for O_3 (~ 0.80), but not for the rest of trace gases ($R \sim 0.10$–0.30). When comparing daily values for CO the agreement improves ($R \sim 0.50$), suggesting that the IASI sensor could moderately capture the day-to-day concentration variations but not the intra-day variability. The scatter (1σ) of the differences between IASI and FTS observations, which can be used as a conservative estimate of the IASI uncertainties, is less than ~ 10 % for CO, ~ 3 % for O_3, and between 1 and 2 % for the rest of the trace gases. All of them are within the target uncertainties of the IASI mission (recall Table 2) and seem to be good enough to capture the day-to-day variations for O_3 and CO when comparing to those observed by FTS records at IZO (values also included in Fig. 7 as a reference). The uncertainties reported here agree well with previous validation studies of IASI L2 V5 operational products using different measurement platforms. For example, errors below 5 % have been reported for O_3 (e.g. Viatte et al., 2011; August et al., 2012), between 10 and 15 % for CO (e.g. August et al., 2012), and ~ 2 % for N_2O and CH_4 (García et al.,

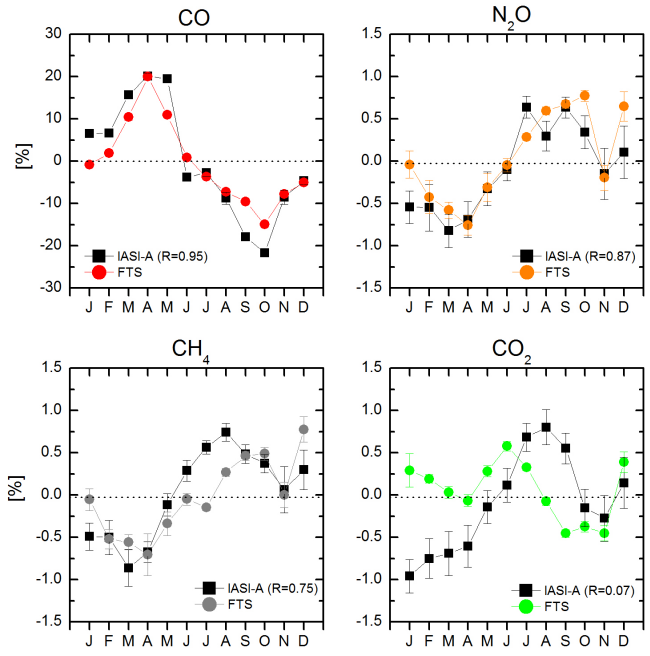

Figure 8. Multi-annual averaged annual cycle for CO, N_2O, CH_4, and CO_2 from IASI-A and FTS observations.

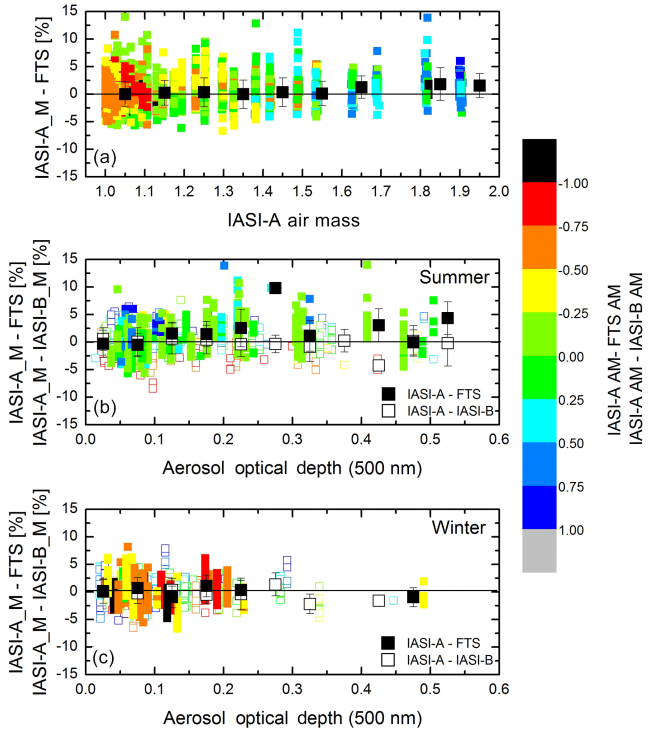

Figure 9. **(a)** Differences between the O_3 de-trended and de-seasonalised variability time series from IASI-A and FTS (in %) as a function of the IASI-A air mass (AM) plotted as black squares with error bar (median and standard deviation per bins of 0.1 of AM), and simultaneous 2-D plot showing the difference between the IASI-A and FTS AMS. **(b)** Same as **(a)** but versus the aerosol optical depth (AOD) at 500 nm, recorded at AERONET SCO station during summer. Also, the differences between IASI-A and IASI-B are included. The black and white squares represent the median and standard deviation per bins of 0.025 of AOD for the IASI-A–FTS and IASI-A–IASI-B differences respectively. **(c)** Same as **(b)** but during winter.

2013). Note that IASI–FTS comparison also confirms the results observed for the consistency study of IASI-A and IASI-B sensors. The correlations and the scatter of the differences observed for both analysis are very similar both at short-term and intra-annual timescales (recall Figs. 6 and 8) with the exception of CO_2. For this trace gas the consistency study reveals a moderate agreement between both IASI sensors (correlations between 0.6 and 0.8 for the annual cycles), but we do not document any agreement for the IASI–FTS comparison (correlation less than 0.2). This is likely due to the degree of maturity of the IASI CO_2 products, as aforementioned. Therefore, the continuous intercomparison of both IASI sensors could successfully be used as a quality control for identifying inconsistencies or instrumental issues in lack of reference ground-based observations.

The differences between the IASI and FTS short-term variability have been analysed as a function of the different parameters, such as the relative horizontal distance between IASI footprints and FTS location, or of the different viewing geometry of the two remote sensing instruments, without identifying significant patterns. As example, the study of viewing geometry is displayed in Fig. 9, where we observe that the differences are uncorrelated to the viewing geometry (IASI-A air mass (Liou, 1980) and difference between IASI-A and FTS AMS). Only the differences for O_3 are displayed as example. However, the same behaviour has been observed for all the trace gases considered.

In addition, the strategic location of IZO allows us to address the IASI–FTS comparison for different atmospheric conditions. Figure 9 also shows the IASI–FTS differences as a function of the aerosol optical depth (AOD) records. This aerosol parameter characterises the total extinction in the line of sight due to atmospheric aerosols and, thus, it can be used as a tracer of Saharan desert air masses in the subtropical North Atlantic region (e.g. García et al., 2012a). To identify these Saharan events, we have considered the AOD observations performed at the Santa Cruz de Tenerife (SCO) station from AERONET network (Holben et al., 1998). SCO, managed by AEMET, is also located on Tenerife, but at sea level ($\approx$ 50 m of altitude) and very close to the sea. Therefore, the SCO AOD records can better quantify the mineral dust outbreaks occurring both in winter (below 2 km of altitude) and in summer (between 2 and 6 km of altitude). Note that although the winter events rarely reach IZO, they will affect the IASI observations including the surrounding ocean. As observed in Fig. 9, during summer, the differences between IASI and FTS observations seem to be

affected by the range of the aerosol load, increasing (absolute value) as the corresponding AOD values increase. This pattern is likely due to the different type of observations: while the FTS measurements are performed from the ground in the direct solar path, the IASI sensors record thermal emission of the Earth–atmosphere from the space and could be more affected by aerosol signatures (thermal emission and scattering processes) (e.g. Vandenbussche et al., 2013; Peyridieu et al., 2013, and references therein). Indeed, when comparing the observations from the two IASI sensors (also displayed in Fig. 9) this difference disappears, which is expected given the very good spectral and radiometric consistency of the two instruments. However, in winter, the IASI–FTS differences seem to be independent on AOD. This fact is likely due to the limited sensitivity of IASI to the boundary layer because of decreasing thermal contrast between the surface and the atmosphere when approaching the surface. In addition to the Saharan conditions, we have also analysed the IASI–FTS comparison under polluted air masses likely coming from North America or Europe (Cuevas et al., 2013, and references therein) by using the intra-day CO concentration variations from the GAW (Global Atmospheric Watch) in situ observations recorded at IZO as a tracer (see Appendix B for details about GAW programme at IZO). No significant patterns were observed (data not shown), but further analysis and longer time series are needed to extract more robust conclusions.

Until now, the IASI–FTS comparison has been addressed in terms of relative variability, but a comparison of absolute TC amounts also provides us useful information. Therefore, to roughly estimate possible biases between IASI-A and FTS observations, the partial column amounts below IZO altitude, computed from the WACCM climatological data, have been added to the FTS observations. By using those data, we find that the IASI observations are consistently lower than FTS observations for all the trace gases, with a median bias (IASI–FTS) of $\sim -6\,\%$ for O_3 and CH_4 (-6.4 and $-5.9\,\%$ respectively) and $\sim -12\,\%$ for N_2O and CO_2 (-12.4 and $-12.1\,\%$ respectively), except for CO. For CO we observe the contrary behaviour; i.e. the IASI sensor overestimates the FTS observations by $\sim 15\,\%$ ($15.2\,\%$). These discrepancies could be partly attributed to systematic IASI and FTS error caused, for example, by the lower IASI sensitivity to the lower troposphere, uncertainties in the IASI ANNs training procedure or in the spectroscopic line parameters. As previously mentioned in Sect. 3, the errors in the spectroscopic line parameters could explain between 2 and $4\,\%$ of the FTS bias, according to our error estimation (see Appendix B). Indeed, experimental intercomparisons between FTS and Brewer observations carried out at IZO in the last years found that FTS systematically overestimates the Brewer O_3 TC amounts by $\sim 4\,\%$ (Schneider et al., 2008; Viatte et al., 2011; García et al., 2012b), which may be due to inconsistencies in the ultraviolet and infrared spectroscopic parameters. This implies that the IASI O_3 observations should have less bias with respect to the actual O_3 concentrations (less than $2\,\%$). However, for CO, the bias obtained is likely introduced by the WACCM estimation since previous studies comparing to other space-based CO products, like the MOPITT sensor (August et al., 2012), or to dedicated IASI CO retrievals, like the FORLI-CO algorithm (Kerzenmacher et al., 2012), found biases lower than $7\,\%$ for regions with low background CO concentrations such as the Atlantic Ocean.

7 Conclusions

This paper documents, for the first time, the uncertainty and the long-term consistency of all EUMETSAT/IASI trace gas products at the same time and using a unique measurement technique as reference, the ground-based FTS experiment.

Firstly, we show that the EUMETSAT/IASI trace gas observations, from both Metop-A/IASI and Metop-B/IASI, are consistent; i.e. neither drifts in time nor were biases found. Therefore, the observations from both remote sensing instruments could be merged to obtain a unique IASI database. Secondly, we focus on the IASI versus ground-based FTS measurement comparison. IASI adequately captures the day-to-day TC variation, the annual cycle, and the long-term trend for its operational products O_3 and CO, as compared to ground-based FTS measurements. Likewise, for N_2O and CH_4 (trace gases with a rather small day-to-day variability), IASI observations can successfully be used to describe their seasonality and interannual trend. However, for CO_2 an acceptable agreement is only achieved at the long-term scale. For the latter three gases, disseminated as aspirational products, improvements in the EUMETSAT retrieval algorithms are currently being carried out to include mature algorithms from the wider scientific community. FORLI-CO and FORLI-O_3 are also being included in the operational IASI L2 suite (Clerbaux et al., 2009). The same methodology can be applied to the upgraded products to support their monitoring in the long term and in view of the expectation of a continued data record from IASI on Metop-C.

This consistency and quality assessment has been carried out using the ground-based FTS located at the IZO and, thus, it is valid for the subtropical North Atlantic region under free troposphere conditions. Although this quality documentation can be used as a benchmark for studies that apply EUMETSAT/IASI trace gas products in climate research, further comparison studies covering other regions might be desirable in order to analyse the possible impact of latitude or other environments, such as urban-industrial or biomass burning areas, on the IASI products accuracy.

Finally, this paper highlights the potential of ground-based FTS experiments once again as an indispensable reference for validating the current space-based observations as well as those anticipated from the next generation of satellite sensors.

Appendix A: Theoretical error estimation of the FTS products

Theoretically, the error of the different FTS products can be estimated by following the formalism detailed by Rodgers (2000), where the difference between the retrieved state, $\hat{\boldsymbol{x}}$, and the real state, $\boldsymbol{x}$, can be written as a linear combination of the a priori state, $\boldsymbol{x}_a$, the real and estimated model parameters, $\boldsymbol{b}$ and $\hat{\boldsymbol{b}}$ respectively and the measurement noise $\boldsymbol{\epsilon}$:

$$(\hat{\boldsymbol{x}} - \boldsymbol{x}) = (\mathbf{A} - \mathbf{I})(\boldsymbol{x} - \boldsymbol{x}_a) + \mathbf{G}\mathbf{K}_b(\boldsymbol{b} - \hat{\boldsymbol{b}}) + \mathbf{G}\boldsymbol{\epsilon}, \quad \text{(A1)}$$

where $\mathbf{G}$ represents the gain matrix, $\mathbf{K}_b$ a sensitivity matrix to model parameters, $\mathbf{I}$ the identify matrix, and $\mathbf{A}$ the averaging kernel matrix. $\mathbf{A}$ relates the real variability to the measured variability of the considered atmospheric state and, thus, represents the way in which the remote sensing system smoothes the real vertical profiles (Rodgers, 2000). Therefore, Eq. (A1) defines three types of error: the first term is the smoothing error associated with the limited vertical sensitivity of the FTS instruments, the second one represents the errors due to uncertainties in the input/model parameters (instrumental characteristics, spectroscopy data), and the third one corresponds to the measurement noise).

The theoretical error estimation strongly depends on the assumed uncertainties. In our case, we consider the error sources and values listed in Table A1 for the input parameters, which are the leading error sources affecting the different FTS products, identified from our experience and the literature (Schneider and Hase, 2008; Sepúlveda et al., 2014, and references therein), while the smoothing error is calculated as $(\mathbf{A} - \mathbf{I})\mathbf{S}_a\ (\mathbf{A} - \mathbf{I})^T$, where $\mathbf{S}_a$ matrix is the is the covariance matrix of the target gas. Strictly, to estimate the smoothing error contribution, the covariance matrix of a real ensemble of atmospheric states must be known (Rodgers, 2000). However, due to lack of real observations of the vertical profiles of all the trace gas considered at IZO, the $\mathbf{S}_a$ for each target gas is assumed and calculated from the WACCM-V6 model estimates. WACCM is a global chemistry model of well-recognised prestigious that has widely demonstrated its ability to provide reliable estimations of the vertical profiles of trace gases and their expected concentration variations (Pan and Brasseur, 2006; SPARC Report, 2010; Smith et al., 2011; Brakebusch et al., 2013). Therefore, here the $\mathbf{S}_a$ is calculated considering the variance of the corresponding gas concentrations at each altitude from the WACCM-V6 climatological data and a Gaussian distribution of strength 5 km for the inter-layer correlation. Note that the total error values are calculated as the root sum squares of all the error sources considered, where the contribution of each error source has been split into statistical and systematic contributions. The exceptions are the spectroscopic parameters and the measurement noise, which are considered as purely systematic and statistical respectively. This error estimation has been applied to the IZO FTS observations between 2010 and 2014 (period studied in the current work).

Table A1. Error sources used for the theoretical error estimation for all the FTS products (chann.: channeling; eff.: efficiency; err.: error; int.: intensity; ν-scale: spectral position; S: intensity; γ: pressure broadening parameter). The second column gives the assumed error value and the third column the partitioning of this error between statistical (ST) and systematic (SY) contributions (Sepúlveda et al., 2014).

Error source	Error	ST/SY
Baseline (chann. and offset)	0.1 and 0.1 %	50/50
Modulation eff. and phase err.	1 % and 0.01 rad	50/50
Temperature profile	2–5 K	70/30
Line of sight	0.1°	90/10
Solar lines (int. and ν-scale)	1 % and 10^{-6}	80/20
Spectroscopy	2 % for S and 5 % γ	0/100

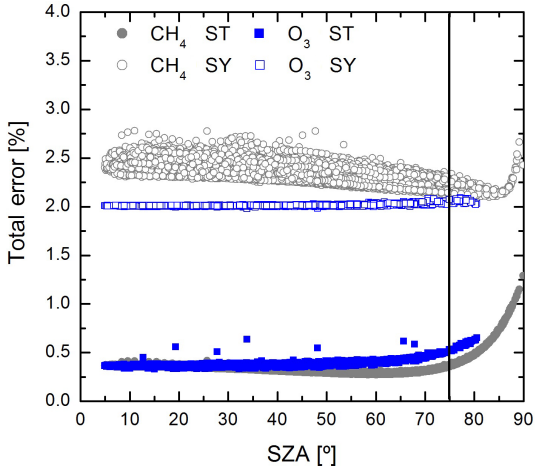

Figure A1. Total statistical (ST) and systematic (SY) errors (in %) as a function of the solar zenith angle (SZA, in °) for FTS O_3 and CH_4 measurements between 2010 and 2014. The black solid line represents the limit value of SZA = 75°. Beyond this value the FTS observations are discarded.

The FTS total errors (statistical and systematic) depend on the observing geometry at which FTS observations are carried out. As illustrated in Fig. A1, the larger theoretical errors are found at high solar zenith angles (SZAs), mainly due to the fact that the FTS observations are more sensitive to possible misalignments of the solar tracker at these SZAs. Therefore, these data (SZA > 75°) are excluded from the study to avoid unrealistic FTS retrievals in the FTS-IASI intercomparison, which represent between 1 % for CO and 8 % for N_2O, CH_4, and CO_2. Considering the filtered FTS observations, the total statistical errors (medians and $\pm 1\sigma$) are 0.40 ± 0.03 % for O_3, 0.50 ± 0.01 % for CO, 0.20 ± 0.03 % for N_2O, 0.30 ± 0.03 % for CH_4, and 0.60 ± 0.14 % for CO_2. The major error sources for the tropospheric gases (N_2O, CH_4, CO_2, and CO) are the baseline uncertainties and the measurement noise, while the uncertainties in the FTS's instrumental line shape (described by the modulation efficiency

and the phase error) dominate the statistical errors for the stratospheric gas O_3. For all the target gases, the systematic error budget is lead by the spectroscopic errors, with median values and $\pm 1\sigma$ of 2.00 ± 0.01 % for O_3, 2.10 ± 0.04 % for CO, 2.10 ± 0.01 % for N_2O, 2.35 ± 0.01 % for CH_4, and 3.50 ± 0.04 % for CO_2.

Appendix B: Collocation criteria between IASI and ground-based FTS observations

To define the temporal collocation, we first estimate the intra-day concentration variations of the target gases and, then, analyse whether the FTS system is good enough to detect this variability by comparing to the respective FTS uncertainties. To do so and to be independent from the FTS observations, we use the high-frequency and high-quality data routinely measured by different in situ analyzers and Brewer spectrometers at IZO.

Ground-level in situ atmospheric continuous measurements of CO_2 (since 1984), CH_4 (since 1984), CO (since 2008), and N_2O (since 2007) have been routinely carried out at IZO as a contribution of AEMET to the WMO GAW programme (Cuevas et al., 2015). The high quality of these measurements has been externally assessed by (1) periodic audits performed in 2004 (CH_4), 2008 (N_2O; Scheel, 2009), 2009 (CO, CH_4, and N_2O; Zellweger et al., 2010, and references therein), and 2013–2014 (CO, CH_4, CO_2, and N_2O, report in preparation) by the World Calibration Centre for Surface Ozone, Carbon Monoxide, Methane and Carbon Dioxide (WCC-Empa), and the World Calibration Centre for Nitrous Oxide (WCC-N_2O); (2) the participation in WMO Round Robin intercomparisons (e.g. WMO Round Robin 5, www.esrl.noaa.gov/gmd/ccgg/wmorr/wmorr_results.php); and (3) the continuous comparison to simultaneous weekly discrete data (Gómez-Peláez et al., 2012, 2013) obtained by the NOAA analysis of weekly collected flask samples, within the NOAA/ESRL/GMD CCGG cooperative air sampling network (www.esrl.noaa.gov/gmd/ccgg/flask.php). The expected uncertainties in these IZO continuous atmospheric measurements are ± 0.1 ppm for CO_2, ± 2 ppb for CH_4, ± 0.2 ppb for N_2O, and ± 2 ppb for CO. Refer to Gómez-Peláez and Ramos (2011), Gómez-Peláez et al. (2012) and Gómez-Peláez et al. (2013) for more details about the measurements and the techniques used. Regarding O_3, we use the daytime O_3 TC observations performed by Brewer spectrometers at IZO since 1991. Like the FTS measurements, the Brewer O_3 data are part of NDACC since 2001. Furthermore, since 2003 they are the Regional Brewer Calibration Center for Europe (www.rbcc-e.org) of the WMO GAW. This guarantees the high quality of their measurements (better than 1 %; Redondas et al., 2014, and references therein).

The intra-day concentration variations have been estimated through the intra-day variation coefficient (VC), calculated as the daily standard deviation divided by the daily mean of the corresponding observations, considering daytime Brewer measurements for O_3 and night-time GAW hourly mole fractions means for the rest of the gases (20:00–08:00 UTC). Note that the IZO in situ night-time data represent the background regional signal of the free troposphere well, while during daytime thermally driven up-slope flow from maritime boundary layer can reach the station and, thus, the in situ data are not well suited for comparing to remote sensing observations. By considering the available time series of these observations since the IASI data are operationally disseminated, i.e. 2008–2013 (see Fig. B1 for CH_4 and O_3), we have estimated the following typical intra-day VC (medians and $\pm 1\sigma$): 0.63 ± 0.52 % for O_3, 2.90 ± 2.65 % for CO, 0.08 ± 0.02 % for N_2O, 0.29 ± 0.17 % for CH_4, and 0.05 ± 0.07 % for CO_2. When comparing experimental and theoretical FTS uncertainties (recall Table 3) to these values, we observe that for CO and O_3 the intra-day VC is larger or much larger than the FTS uncertainty and, therefore, the individual FTS measurements (or hourly medians) should be considered to ensure optimal temporal collocation. Likewise, for CH_4, N_2O, and CO_2, daily medians of the FTS observations can be taken without losing information or affecting the validation results (FTS uncertainty is larger than or comparable to the typical intra-day VC). Note that the remaining concentration variations within the defined temporal window have to be considered when performing the IASI–FTS intercomparison. For CO the hourly VC, considering only night-time observations, is estimated to be 0.98 ± 1.43 %, while for O_3 it is 0.31 ± 0.37 %.

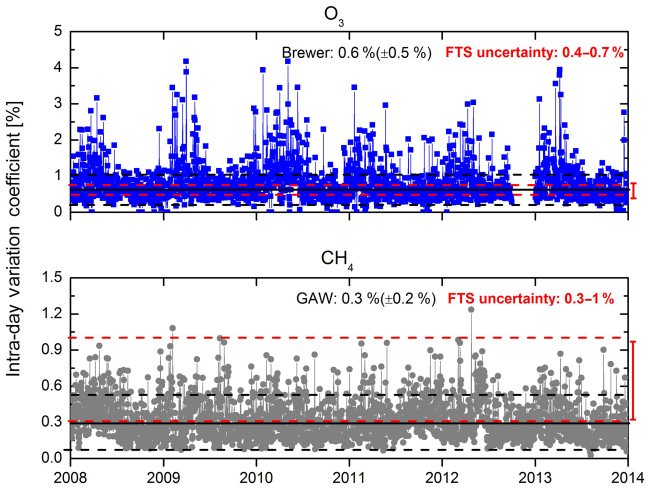

Figure B1. Intra-day variation coefficient (VC) for O_3 total column and in situ CH_4 (in %]) as observed by a Brewer spectrometer and a GAW in situ GC-FID analyzer respectively between 2008 and 2013. The solid and dashed black lines represent the median and $\pm 1\sigma$ of the reference intra-day VC respectively, and the dashed red lines represent the range of theoretical and experimental FTS errors.

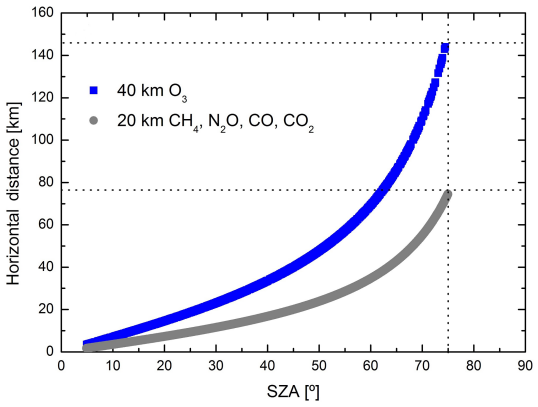

Figure B2. Horizontal distance covered by the FTS observations (in km) versus the solar zenith angle (SZA; in °), at which they are taken for all the target gases. The dashed lines represent the maximal horizontal distances.

As for the temporal collocation, the spatial coincidence criteria have to take into account the spatial concentration variations of each trace gas and the maximal horizontal distance covered by the FTS observations. Since the FTS measurements are performed in the direct solar path, the horizontal projection of the air masses probed by the FTS can be easily calculated from the actual solar observing geometry and the effective altitude of the vertical column observed by the FTS. The latter has been defined as the altitude at which 95 % of the corresponding TC amount is observed and, thus, varies from gas to gas. These effective altitudes have been determined by using the WACCM-V6 climatological data and are $\sim$ 40 km for O_3 and $\sim$ 20 km for the rest of gases, resulting in a maximal horizontal distance of $\sim$ 150 km for O_3 and $\sim$ 80 km for the rest of gases (see Fig. B2).

Regarding the spatial concentration variations of each trace gas, we should consider that IZO is far away from the target gas sources/sinks and embedded in the free troposphere, thereby usually affected by long-range transports of aged and well-mixed air masses (e.g. Cuevas et al., 2013, and references therein). In addition, the latitudinal/longitudinal gradients of the trace gases considered here are rather smooth at oceanic subtropical latitudes. Indeed, the latitudinal relative difference of CO_2 between the Equator and 60° N in 2012 was smaller than 2.5 % (WDCGG, 2014), leading to a mean CO_2 gradient smaller than 0.04 % per degree of latitude. For CH_4 and CO, the latitudinal relative difference between the means of the latitudinal bands 0–30 and 30–60° N in 2012 was smaller than 3.8 and 40 % respectively (WDCGG, 2014). This implies mean CH_4 and CO gradients smaller than 0.13 and 1.3 % per degree of latitude respectively. In the previous three gradient estimations, we have also taken into account the seasonal cycles, which depend on latitude (i.e. we are not simply considering the annual mean latitudinal gradients). For N_2O, the latitudinal relative difference between 20 and 40° N is smaller than 0.32 % (Huang et al., 2008; Kort et al., 2011) and the seasonal cycle is insignificant as can be seen in WDCGG (2014). This implies a mean N_2O gradient smaller than 0.016 % per degree of latitude. For O_3 a gradient of 0.92 % per degree of latitude could be expected at the IZO latitude (value obtained from the ozone observations in 2012 of the space-based Ozone Monitoring Instrument (OMI); Veefkind et al., 2006). Therefore, assuming constant latitudinal gradients within the box ±1° latitude/longitude centred at IZO, the spatial concentration variations inside the box (defined in an equivalent way as the temporal intra-day VC) are expected to be 0.53 % for O_3, 0.75 % for CO, 0.01 % for N_2O, 0.08 % for CH_4, and 0.023 % for CO_2 (where we have taken into account that the standard deviation, in a segment of length 2°, of a linear function with slope Gr per degree, is equal to $\mathrm{Gr}/\sqrt{3}$). These spatial VC are similar (for O_3 and CO) or much smaller (for the rest of trace gases) than the statistical uncertainties of the FTS (recall Table 3). Therefore, no significant concentration variations might be expected within the actual area probed by the FTS observations and, indeed, a slightly wider range than this can be applied for collocating IASI measurements without affecting the validation results. Thus, we define a validation box of ±1° centred at IZO location (i.e. $\pm \sim 110$ km at IZO latitude) for all the trace gases. Previous studies at IZO latitudes found no significant impact of the spatial co-location criteria (50–100 km) on the differences between IASI and FTS TCs for N_2O, CH_4, or CO (Kerzenmacher et al., 2012; García et al., 2013).

Acknowledgements. The research leading to these results has received funding from the Ministerio de Economía y Competitividad from Spain for the project CGL2012-37505 (NOVIA project) and from EUMETSAT under the Fellowship Programme (VALIASI project). Furthermore, M. Schneider, S. Barthlott, A. Wiegele, and Y. González are supported by the European Research Council under FP7/(2007–2013)/ERC grant agreement no. 256961 (MUSICA project).

Edited by: A. Kokhanovsky

References

Alonso-Pérez, S., Cuevas, E., and Querol, X.: Objective identification of synoptic meteorological patterns favouring African dust intrusions into the marine boundary layer of the subtropical eastern north Atlantic region, Meteorol. Atmos. Phys., 113, 109–124, 2011.

Angelbratt, J., Mellqvist, J., Blumenstock, T., Borsdorff, T., Brohede, S., Duchatelet, P., Forster, F., Hase, F., Mahieu, E., Murtagh, D., Petersen, A. K., Schneider, M., Sussmann, R., and Urban, J.: A new method to detect long term trends of methane (CH_4) and nitrous oxide (N_2O) total columns measured within the NDACC ground-based high resolution solar FTIR network, Atmos. Chem. Phys., 11, 6167–6183, doi:10.5194/acp-11-6167-2011, 2011.

August, T., Klaes, D., Schlüssel, P., Hultberg, T., Crapeau, M., Arriaga, A., O'Carroll, A., Coppens, D., Munro, R., and Calbet, X.: IASI on Metop-A: Operational Level 2 retrievals after five years in orbit, J. Quant. Spectrosc. Ra., 113, 1340–1371, doi:10.1016/j.jqsrt.2012.02.028, 2012.

Barret, B., De Mazière, M., and Mahieu, E.: Ground-based FTIR measurements of CO from the Jungfraujoch: characterisation and comparison with in situ surface and MOPITT data, Atmos. Chem. Phys., 3, 2217–2223, doi:10.5194/acp-3-2217-2003, 2003.

Barthlott, S., Schneider, M., Hase, F., Wiegele, A., Christner, E., González, Y., Blumenstock, T., Dohe, S., García, O. E., Sepúlveda, E., Strong, K., Mendonca, J., Weaver, D., Palm, M., Deutscher, N. M., Warneke, T., Notholt, J., Lejeune, B., Mahieu, E., Jones, N., Griffith, D. W. T., Velazco, V. A., Smale, D., Robinson, J., Kivi, R., Heikkinen, P., and Raffalski, U.: Using XCO_2 retrievals for assessing the long-term consistency of NDACC/FTIR data sets, Atmos. Meas. Tech., 8, 1555–1573, doi:10.5194/amt-8-1555-2015, 2015.

Blumstein, D., Chalon, G., Carlier, T., Buil, C., Hébert, P., Maciaszek, T., Ponce, G., Phulpin, T., Tournier, B., and Siméoni., D.: IASI instrument: Technical Overview and measured performances, in: Proccedings SPIE, SPIE, Denver, 2004.

Brakebusch, M., Randall, C. E., Kinnison, D. E., Tilmes, S., Santee, M. L., and Manney, G. L.: Evaluation of Whole Atmosphere Community Climate Model simulations of ozone during Arctic winter 2004–2005, 118, 2673–2688, doi:10.1002/jgrd.50226, 2013.

Brasseur, G., Hauglustaine, D., Walters, S., Rasch, P., J.-F.Muller, Granier, C., and Tie, X.: MOZART: A global chemical transport model for ozone and related chemical tracers – Part 1: Model Description, J. Geophys. Res.-Atmos., 103, 28265–28289, doi:10.1029/98JD02397, 1998.

Clerbaux, C., Boynard, A., Clarisse, L., George, M., Hadji-Lazaro, J., Herbin, H., Hurtmans, D., Pommier, M., Razavi, A., Turquety, S., Wespes, C., and Coheur, P.-F.: Monitoring of atmospheric composition using the thermal infrared IASI/MetOp sounder, Atmos. Chem. Phys., 9, 6041-6054, doi:10.5194/acp-9-6041-2009, 2009.

Crevoisier, C., Chédin, A., Matsueda, H., Machida, T., Armante, R., and Scott, N. A.: First year of upper tropospheric integrated content of CO_2 from IASI hyperspectral infrared observations, Atmos. Chem. Phys., 9, 4797–4810, doi:10.5194/acp-9-4797-2009, 2009a.

Crevoisier, C., Nobileau, D., Fiore, A. M., Armante, R., Chédin, A., and Scott, N. A.: Tropospheric methane in the tropics – first year from IASI hyperspectral infrared observations, Atmos. Chem. Phys., 9, 6337–6350, doi:10.5194/acp-9-6337-2009, 2009b.

Crevoisier, C., Nobileau, D., Armante, R., Crépeau, L., Machida, T., Sawa, Y., Matsueda, H., Schuck, T., Thonat, T., Pernin, J., Scott, N. A., and Chédin, A.: The 2007–2011 evolution of tropical methane in the mid-troposphere as seen from space by MetOp-A/IASI, Atmos. Chem. Phys., 13, 4279–4289, doi:10.5194/acp-13-4279-2013, 2013.

Crevoisier, C., Clerbaux, C., Guidard, V., Phulpin, T., Armante, R., Barret, B., Camy-Peyret, C., Chaboureau, J.-P., Coheur, P.-F., Crépeau, L., Dufour, G., Labonnote, L., Lavanant, L., Hadji-Lazaro, J., Herbin, H., Jacquinet-Husson, N., Payan, S., Péquignot, E., Pierangelo, C., Sellitto, P., and Stubenrauch, C.: Towards IASI-New Generation (IASI-NG): impact of improved spectral resolution and radiometric noise on the retrieval of thermodynamic, chemistry and climate variables, Atmos. Meas. Tech., 7, 4367–4385, doi:10.5194/amt-7-4367-2014, 2014.

Cuevas, E., González, Y., Rodríguez, S., Guerra, J. C., Gómez-Peláez, A. J., Alonso-Pérez, S., Bustos, J., and Milford, C.: Assessment of atmospheric processes driving ozone variations in the subtropical North Atlantic free troposphere, Atmos. Chem. Phys., 13, 1973–1998, doi:10.5194/acp-13-1973-2013, 2013.

Cuevas, E., Milford, C., Bustos, J. J., del Campo-Hernández, R., García, O. E., García, R. D., Gómez-Peláez, A. J., Ramos, R., Redondas, A., Reyes, E., Rodríguez, S., Romero-Campos, P. M., Schneider, M., Belmonte, J., Gil-Ojeda, M., Almansa, F., Alonso-Pérez, S., Barreto, A., González-Morales, Y., Guirado-Fuentes, C., López-Solano, C., Afonso, S., Bayo, C., Berjón, A., Bethencourt, J., Camino, C., Carreño, V., Castro, N. J., Cruz, A. M., Damas, M., De Ory-Ajamil, F., García, M. I., Fernández-de Mesa, C. M., González, Y., Hernández, C., Hernández, Y., Hernández, M. A., Hernández-Cruz, B., Jover, M., Kühl, S. O., López-Fernández, R., López-Solano, J., Peris, A., Rodríguez-Franco, J. J., Sálamo, C., Sepúlveda, E., and Sierra, M.: Izaña Atmospheric Research Center Activity Report 2012–2014, State Meteorological Agency (AEMET), Madrid, Spain, and World Meteorological Organization (WMO), Geneva, Switzerland, nIPO: 281-15-004-2, WMO/GAW Report No. 219, available at: http://izana.aemet.es, last access: 1 December 2015.

Díaz, A. M., Díaz, J. P., Expósito, F. J., Hernández-Leal, P. A., Savoie, D., and Querol, X.: Air masses and aerosols chemical components in the free troposphere at the subtropical Northeast Atlantic region, J. Atmos. Chem., 53, 63–90, 2006.

Dubravica, D., Birk, M., Hase, F., Loos, J., Palm, M., Sadeghi, A., and Wagner, G.: Improved spectroscopic parameters of methane in the MIR for atmospheric remote sensing, in: High Resolution Molecular Spectroscopy 2013 meeting, 25–30 August 2013, Budapest, Hungary, available at: http://lmsd.chem.elte.hu/hrms/abstracts/D16.pdf (last access: 1 December 2015), 2013.

García, O. E., Díaz, J. P., Expósito, F. J., Díaz, A. M., Dubovik, O., Derimian, Y., Dubuisson, P., and Roger, J.-C.: Shortwave radiative forcing and efficiency of key aerosol types using AERONET data, Atmos. Chem. Phys., 12, 5129–5145, doi:10.5194/acp-12-5129-2012, 2012a.

García, O. E., Schneider, M., Redondas, A., González, Y., Hase, F., Blumenstock, T., and Sepúlveda, E.: Investigating the long-term evolution of subtropical ozone profiles applying ground-based FTIR spectrometry, Atmos. Meas. Tech., 5, 2917–2931, doi:10.5194/amt-5-2917-2012, 2012b.

García, O. E., Schneider, M., Hase, F., Blumenstock, T., Wiegele, A., Sepúlveda, E., and Gómez-Peláez, A.: Validation of the IASI operational CH_4 and N_2O products using ground-based Fourier Transform Spectrometer: Preliminary results at the Izaña Observatory (28° N, 17° W), Ann. Geophys.-Italy, 56, doi:10.4401/ag-6326, 2013.

García, O. E., Schneider, M., Hase, F., Blumenstock, T., Sepúlveda, E., Gómez-Peláez, A., Barthlott, S., Dohe, S., González, Y., Meinhardt, F., and Steinbacher, M.: Monitoring of N_2O by ground-based FTIR: optimisation of retrieval strategies and comparison to GAW in-situ observations, NDACC-IRWG/TCCON Meeting, Bad Sulza, Germany, available at: http://www.novia.aemet.es (last access: 1 December 2015), 2014.

García, R. D., García, O. E., Cuevas, E., Cachorro, V. E., Romero-Campos, P. M., Ramos, R., and de Frutos, A. M.: Solar radiation measurements compared to simulations at the BSRN Izaña station, Mineral dust radiative forcing and efficiency study, J. Geophys. Res., 119, 179–194, doi:10.1002/2013JD020301, 2014.

Gisi, M., Hase, F., Dohe, S., and Blumenstock, T.: Camtracker: a new camera controlled high precision solar tracker system for FTIR-spectrometers, Atmos. Meas. Tech., 4, 47–54, doi:10.5194/amt-4-47-2011, 2011.

Gómez-Peláez, A. J. and Ramos, R.: Improvements in the Carbon Dioxide and Methane Continuous Measurement Programs at Izaña Global GAW Station (Spain) during 2007–2009, in: 15th WMO/IAEA Meeting of Experts on Carbon Dioxide, Other Greenhouse Gases, and Related Tracer Measurement Techniques, Jena, Germany, 7–10 September, 2009, GAW Report No. 194, 133–138, World Meteorological Organization, Jena, Germany, 2011.

Gómez-Peláez, A. J., Ramos, R., Gómez-Trueba, V., Campo-Hernández, R., Dlugokencky, E., and Conway, T.: New improvements in the Izaña (Tenerife, Spain) global GAW station in-situ greenhouse gases measurement program, in: 16th WMO/IAEA Meeting on Carbon Dioxide, Other Greenhouse Gases, and Related Measurement Techniques (GGMT-2011), Wellington, New Zealand, 25–28 October 2011, GAW Report No. 206, 76–81, World Meteorological Organization, Wellington, New Zealand, 2012.

Gómez-Peláez, A. J., Ramos, R., Gomez-Trueba, V., Novelli, P. C., and Campo-Hernandez, R.: A statistical approach to quantify uncertainty in carbon monoxide measurements at the Izaña global GAW station: 2008–2011, Atmos. Meas. Tech., 6, 787–799, doi:10.5194/amt-6-787-2013, 2013.

Hase, F.: Improved instrumental line shape monitoring for the ground-based, high-resolution FTIR spectrometers of the Network for the Detection of Atmospheric Composition Change, Atmos. Meas. Tech., 5, 603–610, doi:10.5194/amt-5-603-2012, 2012.

Hase, F., Blumenstock, T., and Paton-Walsh, C.: Analysis of the instrumental line shape of high-resolution Fourier transform IR spectrometers with gas cell measurements and new retrieval software, Appl. Optics, 38, 3417–3422, 1999.

Hase, F., Hanningan, J. W., Coffey, M. T., Goldman, A., Höfner, M., Jones, N. B., Rinsland, C. P., and Wood, S. W.: Intercomparison of retrieval codes used for the analysis of high-resolution ground-based FTIR measurements, J. Quant. Spectrosc. Ra., 87, 25–52, 2004.

Herbin, H., Hurtmans, D., Clerbaux, C., Clarisse, L., and Coheur, P.-F.: $H_2^{16}O$ and HDO measurements with IASI/MetOp, Atmos. Chem. Phys., 9, 9433–9447, doi:10.5194/acp-9-9433-2009, 2009.

Holben, B., Eck, T., Slutsker, I., Tanré, D., Buis, J., Setzer, A., Vermote, E., Reagan, J., Kaufman, Y., Nakajima, T., Lavenu, F., Jankowiak, I., and Smirnov, A.: AERONET-A Federated Instrument Network and Data Archive for Aerosol Characterization, Remote Sens. Environ., 66, 1–16, doi:10.1016/S0034-4257(98)00031-5, 1998.

Huang, J., Golombek, A., Prinn, R., Weiss, R., Fraser, P., Simmonds, P., Dlugokencky, E. J., Hall, B., Elkins, J., Steele, P., Langenfelds, R., Krummel, P., Dutton, G., and Porter, L.: Estimation of regional emissions of nitrous oxide from 1997 to 2005 using multinetwork measurements, a chemical transport model, and an inverse method, J. Geophys. Res., 113, D17313, doi:10.1029/2007JD009381, 2008.

IASI Level 2 Product Guide: EUM/OPSEPS/MAN/04/0033, EUMETSAT, available at: www.eumetsat.int (last access: 1 December 2015), 2012.

Keim, C., Eremenko, M., Orphal, J., Dufour, G., Flaud, J.-M., Höpfner, M., Boynard, A., Clerbaux, C., Payan, S., Coheur, P.-F., Hurtmans, D., Claude, H., Dier, H., Johnson, B., Kelder, H., Kivi, R., Koide, T., López Bartolomé, M., Lambkin, K., Moore, D., Schmidlin, F. J., and Stübi, R.: Tropospheric ozone from IASI: comparison of different inversion algorithms and validation with ozone sondes in the northern middle latitudes, Atmos. Chem. Phys., 9, 9329–9347, doi:10.5194/acp-9-9329-2009, 2009.

Kerzenmacher, T., Dils, B., Kumps, N., Blumenstock, T., Clerbaux, C., Coheur, P.-F., Demoulin, P., García, O., George, M., Griffith, D. W. T., Hase, F., Hadji-Lazaro, J., Hurtmans, D., Jones, N., Mahieu, E., Notholt, J., Paton-Walsh, C., Raffalski, U., Ridder, T., Schneider, M., Servais, C., and De Mazière, M.: Validation of IASI FORLI carbon monoxide retrievals using FTIR data from NDACC, Atmos. Meas. Tech., 5, 2751–2761, doi:10.5194/amt-5-2751-2012, 2012.

Kort, E. A., Patra, P. K., Ishijima, K., Daube, B. C., Jiménez, R., Elkins, J., Hurst, D., Moore, F. L., Sweeney, C., and Wofsy, S. C.: Tropospheric distribution and variability of N_2O: Evidence for strong tropical emissions, Geophys. Res. Lett., 38, L15806, doi:10.1029/2011GL047612, 2011.

Lanzante, J. R.: Resistant, robust and non-parametric techniques or the anayliss of climate data: theory and examples, including ap-

plications to historical radiosonde station data, Internation Journal of Climatology, 16, 1197–1226, 1996.

Liou, K.: An Introduction to Atmospheric Radiation, Academic Press Inc., San Diego, California, USA, p. 58, 1980.

Long, C. and Ackerman, T.: Identification of clear skies from broadband pyranometer measurements and calculation of downwelling shortwave cloud effects, J. Geophys. Res., 105, 15609–15626, doi:10.1029/2000JD900077, 2000.

Matricardi, M. and Saunder, R.: Fast radiative transfer model for simulation of infrared atmospheric sounding interferometer radiances, Appl. Optics, 38, 5679–5691, doi:10.1364/AO.38.005679, 1999.

Pan, L. L., Wei, J. C., Kinnison, D., Garcia, R. R., Wuebbles, D. J., and Brasseur, G.: A set of diagnostics for evaluating chemistry-climate models in the extratropical tropopause region, J. Geophys. Res., 112, D09316, doi:10.1029/2006JD007792, 2006.

Peyridieu, S., Chédin, A., Capelle, V., Tsamalis, C., Pierangelo, C., Armante, R., Crevoisier, C., Crépeau, L., Siméon, M., Ducos, F., and Scott, N. A.: Characterisation of dust aerosols in the infrared from IASI and comparison with PARASOL, MODIS, MISR, CALIOP, and AERONET observations, Atmos. Chem. Phys., 13, 6065–6082, doi:10.5194/acp-13-6065-2013, 2013.

Prospero, J. M., Ginoux, P., Torres, O., Nicholson, S., and Gill, T.: Environmental characterization of global sources of atmospheric soil dust derived from the NIMBUS7 (TOMS) absorbing aerosol product, Rev. Geophys., 40, 1–31, doi:10.1029/20000GR000095, 2002.

Redondas, A., Evans, R., Stuebi, R., Köhler, U., and Weber, M.: Evaluation of the use of five laboratory-determined ozone absorption cross sections in Brewer and Dobson retrieval algorithms, Atmos. Chem. Phys., 14, 1635–1648, doi:10.5194/acp-14-1635-2014, 2014.

Rodgers, C.: Inverse Methods for Atmospheric Sounding: Theory and Praxis, World Scientific Publishing Co., Singapore, 81–99, 2000.

Rothman, L. S., Gordon, I. E., Barbe, A., Benner, D. C., Bernath, P. F., Birk, M., Boudon, V., Brown, L. R., Campargue, A., Champion, J.-P., Chance, K., Coudert, L. H., Dana, V., Devi, V. M., Fally, S., Flaud, J.-M., Gamache, R. R., Goldmanm, A., Jacquemart, D., Kleiner, I., Lacome, N., Lafferty, W., Mandin, J.-Y., Massie, S. T., Mikhailenko, S. N., Miller, C. E., Moazzen-Ahmadi, N., Naumenko, O. V., Nikitin, A. V., Orphal, J., Perevalov, V. I., A. Perrin, A. P.-C., Rinsland, C. P., Rotger, M., Šimečková, M., Smith, M. A. H., Sung, K., Tashkun, S. A., Tennyson, J., Toth, R. A., Vandaele, A. C., and VanderAuwera, J.: The HITRAN 2008 Molecular Spectroscopic Database, J. Quant. Spectrosc. Ra., 110, 533–572, 2009.

Saunders, R., Matricardi, M., and Brunel, P.: An improved fast radiative transfer model for assimilation of satellite radiance observations, Q. J. Roy. Meteor. Soc., 125, 1407–1425, doi:10.1002/qj.1999.49712555615, 1999.

Sawilowsky, S. and Fahoome, G.: Encyclopedia of Statistics in Behavioral Science, chapter: Friedman's Test, John Wiley and Sons Ltd., doi:10.1002/0470013192.bsa237, 2005.

Scheel, H.: System and Performance Audit for Nitrous Oxide at the Global GAW Station Izaña, Tenerife, Spain, November 2008, WCC-N2O Report 2008/11, available at: http://izana.aemet.es (last access: 1 December 2015), 2009.

Schneider, M. and Hase, F.: Technical Note: Recipe for monitoring of total ozone with a precision of around 1 DU applying mid-infrared solar absorption spectra, Atmos. Chem. Phys., 8, 63–71, doi:10.5194/acp-8-63-2008, 2008.

Schneider, M. and Hase, F.: Optimal estimation of tropospheric H_2O and dD with IASI/METOP, Atmos. Chem. Phys., 11, 11207–11220, doi:10.5194/acp-11-11207-2011, 2011.

Schneider, M., Blumenstock, T., Chipperfield, M. P., Hase, F., Kouker, W., Reddmann, T., Ruhnke, R., Cuevas, E., and Fischer, H.: Subtropical trace gas profiles determined by ground-based FTIR spectroscopy at Izaña (28° N, 16° W): Five-year record, error analysis, and comparison with 3-D CTMs, Atmos. Chem. Phys., 5, 153–167, doi:10.5194/acp-5-153-2005, 2005.

Schneider, M., Hase, F., and Blumenstock, T.: Water vapour profiles by ground-based FTIR spectroscopy: study for an optimised retrieval and its validation, Atmos. Chem. Phys., 6, 811–830, doi:10.5194/acp-6-811-2006, 2006.

Schneider, M., Redondas, A., Hase, F., Guirado, C., Blumenstock, T., and Cuevas, E.: Comparison of ground-based Brewer and FTIR total column O_3 monitoring techniques, Atmos. Chem. Phys., 8, 5535–5550, doi:10.5194/acp-8-5535-2008, 2008.

Schneider, M., Wiegele, A., Hase, F., Barthlott, S., Blumenstock, T., García, O., and E.Sepúlveda: IASI/METOP retrievals within the project MUSICA, IASI Conference 2013, Hyères, France, 4–8 February 2013.

Sepúlveda, E., Schneider, M., Hase, F., García, O. E., Gomez-Pelaez, A., Dohe, S., Blumenstock, T., and Guerra, J. C.: Long-term validation of tropospheric column-averaged CH4 mole fractions obtained by mid-infrared ground-based FTIR spectrometry, Atmos. Meas. Tech., 5, 1425–1441, doi:10.5194/amt-5-1425-2012, 2012.

Sepúlveda, E., Schneider, M., Hase, F., Barthlott, S., Dubravica, D., García, O. E., Gomez-Pelaez, A., González, Y., Guerra, J. C., Gisi, M., Kohlhepp, R., Dohe, S., Blumenstock, T., Strong, K., Weaver, D., Palm, M., Sadeghi, A., Deutscher, N. M., Warneke, T., Notholt, J., Jones, N., Griffith, D. W. T., Smale, D., Brailsford, G. W., Robinson, J., Meinhardt, F., Steinbacher, M., Aalto, T., and Worthy, D.: Tropospheric CH_4 signals as observed by NDACC FTIR at globally distributed sites and comparison to GAW surface in situ measurements, Atmos. Meas. Tech., 7, 2337–2360, doi:10.5194/amt-7-2337-2014, 2014.

Smith, K., Atlas, E. L., Zhu, X., Pope, L., Lueb, R., Moore, F. L., Miller, B. R., Montzka, S. A., Elkins, J. W., Nance, D., Sweeney, C., Pan, L., Kinnison, D. E., Hendershot, R., Romashkin, P., Wofsy, S. C., Daube, B., Kort, E. A., Jimenez, R., and Pittman, J. V.: Selected trace gas distributions and relationships: a comparison of HIAPER Pole to Pole Observations (HIPPO) and Whole Atmosphere Community Climate Model (WACCM), American Geophysical Union, Fall Meeting 2011, available at: http://adsabs.harvard.edu/abs/2011AGUFM.A11K..02S, 2011.

SPARC Report: SPARC Report on the Evaluation of Chemistry-Climate Models, Report No. 5, WCRP-132, WMO/TD-No. 1526, edited by: Eyring, V., Shepherd, T. G., and Waugh, D. W., available at: http://www.atmosp.physics.utoronto.ca/SPARC, 2010.

Turquety, S., Hadji-Lazaro, J., Clerbaux, C., Hauglustaine, D., Clough, S. A., Cassé, V., Schulüssel, P., and Mégie, G.: Operational trace gas retrieval algorithm for the Infrared Atmo-

spheric Sounding Interferometer, J. Geophys. Res., 109, D21301, doi:10.1029/2004JD004821, 2004.

Vandenbussche, S., Kochenova, S., Vandaele, A. C., Kumps, N., and De Mazière, M.: Retrieval of desert dust aerosol vertical profiles from IASI measurements in the TIR atmospheric window, Atmos. Meas. Tech., 6, 2577–2591, doi:10.5194/amt-6-2577-2013, 2013.

Veefkind, J., de Haan, J., Brinksma, E., Kroon, M., and Levelt, P.: Total Ozone from the Ozone Monitoring Instrument (OMI) Using the DOAS technique, 44, 1239–1244, doi:10.1109/TGRS.2006.871204, 2006.

Velazco, V., Wood, S. W., Sinnhuber, M., Kramer, I., Jones, N. B., Kasai, Y., Notholt, J., Warneke, T., Blumenstock, T., Hase, F., Murcray, F. J., and Schrems, O.: Annual variation of strato-mesospheric carbon monoxide measured by ground-based Fourier transform infrared spectrometry, Atmos. Chem. Phys., 7, 1305–1312, doi:10.5194/acp-7-1305-2007, 2007.

Viatte, C., Schneider, M., Redondas, A., Hase, F., Eremenko, M., Chelin, P., Flaud, J.-M., Blumenstock, T., and Orphal, J.: Comparison of ground-based FTIR and Brewer O_3 total column with data from two different IASI algorithms and from OMI and GOME-2 satellite instruments, Atmos. Meas. Tech., 4, 535–546, doi:10.5194/amt-4-535-2011, 2011.

WDCGG: WMO World Data Center for Greenhouse Gases Data Summary, WDCGG No. 38, Japan Meteorological Agency in cooperation with World Meteorological Organization, 4–42, 2014.

Zellweger, C., Klausen, J. Ã., Buchmann, B., and Scheel, H.: System and Performance Audit of Surface Ozone, Carbon Monoxide, Methane and Nitrous Oxide at the Global GAW Station Izaña, Spain, March 2009, WCC-Empa Report 09/1, availabale at: http://gaw.empa.ch/audits/IZO_2009.pdf, 2010.